

PREDICTING CONCRETE RESISTIVITY FROM OHMS LAW

by

Alex Jay Hammond

A thesis submitted to the faculty of
The University of Utah
in partial fulfillment of the requirements for the degree of

Master of Science

Department of Civil and Environmental Engineering
The University of Utah

May 2010

Copyright © Alex Jay Hammond 2010

All Rights Reserved

THE UNIVERSITY OF UTAH GRADUATE SCHOOL

SUPERVISORY COMMITTEE APPROVAL

of a thesis submitted by

Alex Jay Hammond

This thesis has been read by each member of the following supervisory committee and by majority vote has been found to be satisfactory.

Dr. [Signature]

[Signature]

Dr. [Signature]

Chris Pantelides

Dr. [Signature]

[Signature]

THE UNIVERSITY OF UTAH GRADUATE SCHOOL

FINAL READING APPROVAL

To the Graduate Council of the University of Utah:

I have read the thesis of Alex Jay Hammond in its final form and have found that (1) its format, citations, and bibliographic style are consistent and acceptable; (2) its illustrative materials including figures, tables, and charts are in place; and (3) the final manuscript is satisfactory to the supervisory committee and is ready for submission to The Graduate School.




Alex Jay Hammond
Chair, Supervisory Committee

Approved for the Major Department



[Signature]
[Title]

Approved for the Graduate Council



Charles [Name]
Dean of The Graduate School

ABSTRACT

The resistance of concrete to the penetration of chloride ions from deicing salts or other brine solutions is one of the most important performance properties used in concrete mixture design specifications. This property provides valuable insight into the time to the corrosion initiation of reinforcing steel. The AASHTO T277 or ASTM C1202 tests have been used in the approval of mixture designs for most high performance concrete (HPC) specifications as an indicator of durability. This test is time consuming and not conducive to the volume or time constraints of quality control or quality assurance (QC/QA) testing of in-situ concrete or field cured concrete. In recent years, various iterations of the Wenner probe have been developed to characterize the electrical resistance of concrete, a property that plays an important role in the initiation and propagation of corrosion. Fully developed life cycle analysis models use both a) corrosion initiation time; and b) corrosion propagation components to address their goals. This thesis demonstrates that the physics of these two tests are closely related and using 26 different HPC mixture designs, the electrical resistivity can reliably predict the resistance of concrete to the penetration of chloride ions with substantially less effort and expense. In this large number of different mixture designs for bridge decks and exposed structures, the electrical resistance consistently correlated with the T277 and C1202 test results. In addition, the concrete's electrical resistance is a physical property of the

concrete, not just an indicator of potential behavior. As such, it can be directly used in the development of corrosion models.

This thesis discusses the research conducted to verify the correlation between the ASTM C1202 testing results and the Wenner resistivity results using Ohms law.

Through this research, it was determined that there was a consistent relationship through Ohms law.

TABLE OF CONTENTS

ABSTRACT	iv
LIST OF TABLES	viii
LIST OF FIGURES	ix
ACKNOWLEDGMENTS	xi
Chapter	
1. INTRODUCTION	1
Electrical Conductivity of Concrete and Its Role in Corrosion	1
Tests of Resistivity and Conductivity	2
The Need of the Tests	3
The Need of a Correlation.....	4
Problem Statement	4
2. LITERATURE REVIEW	5
Resistivity and ASTM C1202	5
3. MATERIALS AND METHODS.....	10
Concrete Materials and Methods	10
ASTM C1202	12
Wenner Resistivity	14
4. ACI MANUSCRIPT	18
Manuscript Introduction.....	18
Manuscript	19
5. EVALUATION OF DATA	40
Geometric Correction.....	40
Joule Effect	41

Resistivity from Coulomb and Coulomb from Resistivity	43
Deviation from Theoretical Ohms Law	45
Drying Time and Excluded Data	46
Comparison with Prior Work.....	47
Material Influence Evaluation.....	47
Suggested Additional Research	52
6. SUMMARY AND CONCLUSIONS	59
Summary	59
Conclusions.....	60
APPENDIX.....	63
REFERENCES	66

LIST OF TABLES

<u>Table</u>	<u>Page</u>
3.1 Cementitious material properties	11
3.2 Aggregate material properties.....	11
4.1 Drying time effect on resistivity for 65TI/30F/5SF	25
4.2 Wenner resistivity conversions to coulomb	29
4.3 AASHTO T277 conversions to resistivity	31
5.1 Independent testing of geometric correction factor	41
5.2 Extended testing coulomb vs. joule corrected coulomb	42
5.3 Adjusted equation variation from theoretical equation.....	46
5.4 Correction factor variability.....	57
A.1 Condensed 98-day resistivity and coulomb data	64
A.2 Condensed 28-day resistivity and coulomb data	65

LIST OF FIGURES

<u>Fig.</u>	<u>Page</u>
3.1 Wenner resistivity probes	15
4.1 AASHTO T277 test apparatus	21
4.2 Wenner meter.....	22
4.3 Raw coulomb and adjusted coulomb (joule effect and geometric correction)	32
4.4 Raw coulomb and adjusted T277 coulomb (joule effect).....	33
4.5 Raw coulomb and adjusted (geometric correction) coulomb obtained from resistivity (Wenner meter)	34
4.6 Raw resistivity and adjusted resistivity (joule effect and geometric correction)...	35
4.7 Adjusted resistivity (joule effect) calculated from T277 data	36
4.8 Raw resistivity and adjusted (geometric correction) Wenner resistivity	37
4.9 Wenner resistivity vs. AASHTO T277 coulomb.....	38
4.10 Comparison of adjusted (joule effect and geometric correction) relationship and theoretical relationship	39
5.1 Joule effect.....	43
5.2 Comparison to previous work.....	48
5.3 AASHTO T277 coulomb vs. Wenner resistivity.....	49
5.4 Pozzolan substitution comparison.....	50
5.5 AASHTO T277 coulomb vs. Wenner resistivity – silica fume	51

5.6	AASHTO T277 coulomb vs. Wenner resistivity – metakaolin	52
5.7	AASHTO T277 coulomb vs. Wenner resistivity – slag	53
5.8	AASHTO T277 coulomb vs. Wenner resistivity – Class F fly ash	54
5.9	AASHTO T277 coulomb vs. Wenner resistivity – Class F2 fly ash	55
5.10	AASHTO T277 coulomb vs. Wenner resistivity – Class C fly ash.....	56
5.11	98-day AASHTO T277 coulomb vs. 28-day Wenner resistivity.....	57

ACKNOWLEDGMENTS

I would like to acknowledge contributions from the Federal Highway Administration and the states involved in the pool funded study that made this research possible. Dr. Paul Tikalsky has provided abundant guidance with the research and creation of this thesis and for that I am grateful. Acknowledgment goes to those with whom I worked in the laboratory, including Pratanu Ghosh and the many undergraduates that helped collect the data, and Mark Bryant. I would especially like to thank my wife Amanda and my family for their patience and encouragement along the way.

CHAPTER 1

INTRODUCTION

As a culminating report of work completed at the University of Utah in the Civil and Environmental Engineering department, this thesis is submitted to the department and graduate school. The work encompasses research on a correlation between two testing methods: Wenner resistivity and ASTM C1202 – “Standard Test Method for Electrical Indication of Concrete’s Ability to Resist Chloride Ion Penetration” (1) (also known as American Association of State Highway and Transportation Officials (AASHTO) Standard T277-05, “Standard Method of Test for Electrical Indication of Concrete’s Ability to Resist Chloride”(2)) using established physics principles.

Electrical Conductivity of Concrete and Its Role in Corrosion

The electrical conductivity of concrete plays a major role in the corrosion of steel rebar embedded in concrete. If the concrete has high conductivity, there is a greater potential for corrosion cells to develop due to greater concentrations of ions at the rebar level as opposed to low conductivity concrete. The corrosion of rebar is an electrochemical process, which requires electrochemical potentials to form corrosion cells. These cells are often formed due to different ionic concentrations of alkalis and chlorides within a material. When the metal has different ionic concentrations at

different locations along its length, anodes and cathodes may develop. In order for the corrosion to take place, water, oxygen, and ions need to be present between the cathode and anode. When chlorides are present and with high conductivity concrete (highly permeable), more ions are present for this process to initialize and propagate corrosion. The corrosion that occurs is manifested as the formation of rust, which when it is formed has an expansive reaction. When the rust expands, the concrete is no longer able to withstand the tensile forces and cracks or spalls. Cracking and spalling brings more air, water, and ions that penetrate very quickly when cracks are present, and thus propagate the rusting. Conversely, with low permeable concrete there are less chloride ions present, so the reaction is much slower if it develops at all. This provides a longer lasting structure due to the reduction of corrosion in the rebar.

When the rebar is rolled, its surface has a passivating iron-oxide layer that is resistant to corrosion in an alkaline environment of concrete, pH 13. The introduction of chloride ions reduces the pH of the pore water in concrete. When the pH drops below 10, the coating becomes susceptible to corrosion. The reduction of pH may destroy the protective layer on the rebar and initiate the corrosion process. These reasons are why measuring the electrical conductivity of concrete is important in concrete structures containing steel reinforcement (3).

Tests of Resistivity and Conductivity

The Wenner resistivity testing method was initially developed for use by geologists to determine the resistivity of soil strata; it has since been modified for use in testing certain material properties in concrete (4). This method involves using a 4 probe

device used to measure the electrical resistivity of a material. The use of this device for this purpose is relatively new; only in the last 10 years has it been used for this purpose. The ASTM C 1202 test method has been used since the 1980s as an indicator of the resistance to chloride ion penetration into concrete. The difficulty with the widespread acceptance of this testing method is the lengthy time required to perform the procedures. The curing and sample preparation takes 28 to 56 days and the test requires another 6 hours to perform. This time frame is unacceptable for most quality control measures.

The information gained from performing these tests indicates how resistant the concrete is to chloride ion penetration. Although it is not a direct measurement, it has been shown to be a reliable indicator.

The Need of the Tests

A major reason for premature bridge replacement in the United States is due to rebar corrosion. This corrosion is due to roadway salts being applied during winter or sea salt spraying onto the structure and the chlorides in the salts penetrating the concrete to the rebar. As the rebar corrodes, it expands and delaminates and cracks concrete, which furthers the corrosion process. The importance of the ASTM C1202 testing method is to determine which concrete mixtures can reduce or eliminate chlorides from penetrating the concrete and attacking the rebar. One deficiency in the ASTM C1202 method is the ability to use it in-situ to ensure the concrete placed meets the testing standard.

The Need of a Correlation

One of the major flaws of the existing research in this area is that the researchers simply show a connection between the two testing methods, but do not present a theoretical link between the two tests. Several articles have been published on research showing a relationship between these two testing methods. The importance of this research is to show how they are related using a basic physics concept, Ohms law (5). With this knowledge, it is anticipated that the Wenner resistivity can eventually replace the ASTM C1202 as an electrical indicator of potential chloride ion penetration that can be used in-situ.

Problem Statement

The purpose of this work is to relate the ASTM C1202 testing results with results obtained using a Wenner resistivity device by utilizing Ohms law. Throughout the scientific community, it has been established that there is a correlation in the testing results based on experimental data, but these findings have failed to explain what the relationship is and why there is a relationship. The main objective is to show that there is a scientific connection between the two testing results through Ohms law.

CHAPTER 2

LITERATURE REVIEW

The following literature review can also be found in the journal article submitted to the American Concrete Institute Materials Journal in Chapter 4.

Resistivity and ASTM C1202

Investigation into whether the AASHTO T277 testing method can be used as an indicator for chloride ion penetration was conducted by Feldman et al. (6). It was determined that the physical characteristics of the concrete specimens in the T277 test were changed by the severe conditions found in the test, thus possibly leading to skewed results. They determined that there was good correlation between current passed and conductivity (which is the inverse of resistivity). One of their recommendations was to perform more tests to correlate data between resistivity and initial current in the T277 test with blended cements.

An evaluation of the Wenner technique for measuring resistivity was conducted by Gowers and Millard to evaluate the best testing methods for using the Wenner device (7). Their work consisted of using the Wenner device in various situations to determine the best way to use the device. Their recommendations include ensuring good contact

between the device and the concrete, allowing adequate edge distance, having probe spacing larger than 1.5 times the maximum aggregate size, and using a pachometer to determine bar locations in concrete to avoid bar interference.

Research into the factors involved in performing resistivity readings was investigated by Sengul and Gjorv (8). Through this research, it was verified that the spacing of the resistivity probes on the Wenner four probe array has a large influence on the resistivity measured. This same study showed the temperature and moisture curing conditions of the specimens can change the resistivity outcome. The conclusions of this research indicate that resistivity measurements can be used for quality control as long as the testing method and specimen conditions are uniform between tests.

Research was done on the effect of specimen geometry and probe spacing on resistivity readings by Morris et al. (9). This research was conducted to correlate readings from standard strength test cylinders with semi-infinite slabs in order to indirectly measure concrete characteristics. The experiment involved creating a finite element model of concrete specimens as well as testing specimens with a Wenner resistivity device. A correction factor was developed to correlate experimental and modeled values of resistivity with different probe spacing and specimen shape and size. This correction factor is called the geometric correction factor.

Experimentation using the Wenner device on 529 sample sets was conducted by Kessler et al. at the Florida Department of Transportation (10) to investigate whether resistivity can be used as a quality control measure in place of AASHTO T277 and the variation in readings from different testing technicians was also studied. Their findings indicate that, using the geometric correction factor, there is a good correlation between

AASHTO T277 and resistivity ($R^2=0.948$) and it was suggested as a replacement for AASHTO T277. The Florida Department of Transportation has also developed a method to standardize how resistivity readings should be performed (11).

The T277 test involves the application of 60Vdc, which increases the current flow producing excessive heating of the specimen and changing the pore structure of concrete over a short period of time. This increase in specimen temperature during testing, due to the application of a high voltage, is called the “joule effect.” As a resistor (concrete specimen) is heated, the conductivity of the material increases. Since the AASHTO T277 is a measurement of conductivity, an excessive increase of specimen temperature during testing results in a higher T277 reading, created by the joule effect. A relationship between temperature change during testing and final coulomb readings was developed by Betancourt and Hooton (12) in order to eliminate excessive heating effects of the specimen during testing. These researchers also state that the joule effect has been a major obstacle in connecting T277 data and the electrical conductivity. They recommended that research should be performed to validate the correlation in these two testing methods. The data presented in this paper shows the Wenner resistivity data and AASHTO T277 data are related with consideration of the joule effect.

Investigation into whether the AASHTO T277 test can accurately predict chloride ion ingress with concrete mixtures containing silica fume (SF) and ground granulated blast-furnace slag (GGBFS) using the AASHTO T277 test, AASHTO T259, and resistivity readings was performed by Wee et al. (13). The investigation included varying curing days and material fineness. The findings were that there was a correlation between the AASHTO T277 test and resistivity readings, but the connection between

AASHTO T277 and the AASHTO T259 was not very strong ($R^2=0.40$ for GGBFS and $R^2=0.10$ for SF). The recommendation was that AASHTO T277 is only a predictor of relative chloride ion ingress of mixtures containing SF and GGBFS.

As part of research performed by Smith at Penn State University, two different manufacturers of Wenner resistivity devices were tested to determine the relationship between the two devices, as well as how the data correlates with the AASHTO T277 test (14). The conclusion was the data from the meters follows a similar trend, but does not present the same values for each measurement. For example, in a mixture where the resistivity was moderately high ($34 \text{ k}\Omega\cdot\text{cm}$, $13.4 \text{ k}\Omega\cdot\text{in}$) with one meter was also moderately high ($20 \text{ k}\Omega\cdot\text{cm}$, $7.9 \text{ k}\Omega\cdot\text{in}$) with the other meter, only not as high. Data obtained through Smith's research indicate that there is a relationship between the AASHTO T277 test and resistivity readings. From curves comparing AASHTO T277 data with resistivity using a similar device to the one used in the research reported herein, a good relationship was obtained ($R^2=0.897$). Another important idea that can be gathered through Smith's research is that concrete exposed to chlorides for extended periods of time may have lower resistivity readings than those not exposed to chlorides.

An investigation into the testing methods used to determine concrete chloride penetration was performed for the Federal Highway Administration by Stanish et al. (15). This investigation involved a literature review of the current methods used in 1997 to determine the chloride penetration of concrete. Many methods were investigated in this thorough analysis including the AASHTO T277 (Rapid Chloride Permeability Test) and testing using Resistivity Techniques. The researchers investigated the pros and cons of each test and concluded that each test has its strengths and weaknesses and that the

proper test should be chosen for the desired outcome. The difficulties described for the ASTM C1202 test were concerning current passing through all ions, not just chloride ions; the data was collected before steady state was reached; and the excessive heating of the specimens can cause error. The difficulty with resistivity was concerning the conductivity of the pore solution in the concrete. This could potentially yield different resistivity readings with the same mixture of concrete.

Burke and Hicks (16) used 3 inch by 6 inch specimens submerged in 3% NaCl solution for 2 years for an electrochemical test to determine resistivity of the concrete material. This resistivity was compared to AASHTO T277 data and a relationship was developed. The researchers determined that the relationship developed was adequate for mixtures with permeability values below 2000 coulomb, but above this threshold, the specimens were subject to excess heating during testing, which produced unacceptable results.

CHAPTER 3

MATERIALS AND METHODS

This chapter describes the materials and methods used to create and test the concrete in this study. The concrete materials are only briefly discussed; a more thorough analysis of the concrete materials and admixtures can be found elsewhere as referenced in this chapter.

Concrete Materials and Methods

Mixture Materials

The concrete mixture design was based on 564 pounds of total cementitious materials per cubic yard. The mixture design includes air entrainment, ASTM C33 No. 67 limestone aggregate, and C33 sand with a fineness modulus of 2.81. The coarse and fine aggregate was from a local aggregate provider located in Salt Lake City, Utah. The types of cement used varied from ASTM C595 Type IP (portland-pozzolan), Type IS (portland blast-furnace slab), and Type ISM (slag-modified portland cement), to ASTM C1157 GU. The supplementary materials include ASTM C1140 silica fume, ASTM C618 Class F fly ash, and Class C fly ash, ASTM C618 Class N pozzolan metakaolin, and ASTM C989 Grade 100 ground blast furnace slag. More information on these

materials can be found in the report “Development of Performance Properties of Ternary Mixtures: Phase I Final Report,” report number *Pooled Fund Study TPF-5(117)* by Tikalsky et al. submitted to the Federal Highway Administration (FHWA) in December of 2007 (17). A summary of the material specific gravity for cementitious material can be found in Table 3.1 and specific gravity, absorption, and fineness modulus for aggregate materials in Table 3.2. Additional information on the cementitious material and admixtures can also be found in the journal article “Effects of Different Air Engraining Agents (AEA), Supplementary Cementitious Materials (SCM), and Water Reducing Agent (WR) on the Air Void Structure of Fresh Mortar” by Rupnow et al. (18).

Table 3.1 – Cementitious material properties

Material	Specific Gravity
Type I Cement	3.15
TISM Cement	2.95
TIP Cement	3.11
Limestone Cement	3.25
Class C Fly Ash	2.62
Class F Fly Ash	2.37
Class F Fly Ash	2.41
GGBFS 120	2.96
Silica Fume	2.21
Metakaolin	2.52

Table 3.2 – Aggregate material properties

Material	Specific Gravity	Absorption	Fineness Modulus
Natural River Sand	2.64	1.96%	2.81
¾ inch Gravel	2.68	0.86%	N/A

Mixture Design

Concrete mixtures were made using a 0.44 water-to-cementitious ratio in batch sizes ranging from 1 cubic foot to 3.5 cubic feet. Using the same proportions to make one cubic yard of concrete (quantity more widely used), the approximate weight of coarse aggregate would be 1,811 pounds, fine aggregate weight would be 1,237 pounds, and cementitious material would be 564 pounds.

Mixture Methods and Curing Methods

The concrete was mixed in a 9 cubic foot counter planetary mixer with an energy cycle of 3 minutes on, 3 minutes off, and a final 2 minutes on before discharging the concrete. Smaller mixtures of 1 cubic foot were done in an inclined shaft drum mixer as needed. Cylinders and other testing specimens were cast and cured in accordance with current standards of practice. Resistivity specimens were wet cured in a curing chamber from the time mixed until removal for testing. Chloride ion penetration samples were wet cured for 14 days in water with lime, then removed for dry curing in the laboratory until tested.

ASTM C1202

Curing and Testing

In accordance with ASTM C1202, concrete cylinders were prepared from concrete mixtures with various amounts of pozzolanic materials. These cylinders were wet cured in a curing tank with lime for 14 days before being removed for dry curing and were tested on the 98th day after they were cast. These cylinders, after being wet cured,

were sliced using either a lapidary saw or modified tile saw into 2 inch thick by 4 inch diameter specimens. Once sliced, they were allowed to dry. When dry, epoxy was applied to the outside diameter of the slice. The specimens were allowed to dry for at least 1 week before testing. The testing procedures were done in accordance with ASTM C1202 using a commercially available instrument manufactured for use with the ASTM C1202 testing method.

The specimens were wet cured for 14 days to allow the cement and pozzolans to react and to simulate the curing duration that may be applied on structures in the field. Once removed, they were exposed to laboratory temperatures until the day they were tested.

Equipment

The testing equipment used for testing was a commercially available instrument manufactured for use with the ASTM C1202 testing method. This was a complete testing set up with a power source, testing cells, and all the software needed to collect and compile the data. The software included a data logger that collected the current and temperature of the cells, variability to be able to test the specimens at different voltages and different times, and a report generating system.

Results

The results obtained by using this testing method are in coulombs (Amp*sec), which is an integration of the current applied over the testing time. This coulomb value is then reduced according to ASTM C1202 to an equivalent result that would be obtained

using a specimen diameter of 3.75 inches. The values in ASTM C1202 were established using 3.75 inch diameter specimens, so in order to compare experimental results with the standard in ASTM C1202, this correction should be applied.

Wenner Resistivity

Method

Florida Department of Transportation Method FM 5-578

A summary of FM 5-578 (11) is given for completeness. The testing method FM 5-578 requires three 4.0 inch by 8.0 inch specimens meeting ASTM C470 requirements. All specimens should be moist cured in a moist room (without lime) until the day of testing. Twenty-four hours after being cast, the cylinder molds are removed and four marks are placed at 0, 90, 180, and 270 degrees around the circumference of the top of the cylinder. The cylinders are then placed back in the curing room until the time of testing, at which time the cylinders are removed. The Wenner resistivity probe, with 1.5 inch probe spacing, is then placed with its handle parallel with the center of the cylinder at approximately half the height of the cylinder. The operator then waits 3 to 5 seconds for a stable reading, and then rotates the cylinder to take readings below the 0, 90, 180, and 270 degree marks. These readings are to be done twice per cylinder. Once this is completed, the operator moves on to the next cylinder. When readings have been collected for all three specimens, the readings are averaged to obtain the average resistivity for the mixture.

Testing Method for Data in This Paper

Resistivity readings were done in accordance with the Florida Department of Transportation (FDOT) testing method (FM 5-578) with the exception of the probe spacing, number of cylinders cast, and resistivity characterization for permeability. The data in this report were tested using a probe spacing of 2 inches, instead of 1.5 as recommended by FDOT; and the number of cylinders cast for testing varied from 2 to 6, instead of 3 as recommended. The probe spacing could not be changed as it came from the manufacturer with 2 inch spacing; however, the 2 inch spacing was beneficial as compared to the 1.5 inch spacing because there is less large aggregate interference with the longer spacing. Large aggregate interference occurs when the spacing is not more than 2 times the diameter of the largest aggregate size and with longer spacing there is less interference. Fig. 3.1 shows the different Wenner probes; on the left is the probe used by FDOT and on the right is the one used in this study.

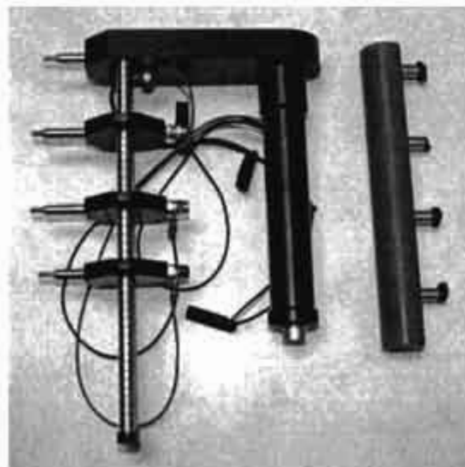


Fig. 3.1—Wenner resistivity probes

Left: Adjustable, Right: Nonadjustable

Curing

Resistivity specimens were cured according to the requirements of FM 5-578, which were to cast the specimens, cure them in a wet curing room in accordance with ASTM C192 until the day of testing, and remove and test the cylinders. No time duration between when the specimen is removed and when it should be tested was specified in the FDOT standard. For this research, the tests were to be completed within 15 minutes of being removed from the curing room. Only specimens or testing results done in accordance with this curing method (unless intentionally cured differently) were used for analysis.

Equipment

The resistivity measuring setup chosen for testing was a commercially available Wenner resistivity meter with a four probe Wenner device with foam contact points and spacing of 2 inches, as shown in Fig. 3.1. The setup was chosen due to the ease of use and it offered several other attachments that could be used for other testing being performed in the lab by others. Other devices, such as those used by the Florida Department of Transportation in which the probe spacing can be adjusted, could have been used, but it is recommended to use the same device for all testing.

Results and Considerations

The results of this testing method are in $\text{k}\Omega\cdot\text{cm}$ and are for a curved concrete surface unless corrected. In order to reduce the variability of the data, some effects were kept constant throughout the testing. These effects include using only 4 inch x 8 inch

cylinders, keeping cylinders in wet cure until day of testing, keeping approximately the same edge distance with probes, using the same meter, testing within 15 minutes of removal from wet cure, and not testing with rebar present. In this way, consistent results could be obtained throughout the mixtures in order to establish a relationship.

CHAPTER 4

ACI MANUSCRIPT

Manuscript Introduction

The journal article found in this chapter beginning on the next page has been submitted to the American Concrete Institute (ACI) Materials Journal for acceptance in February 2010, and is currently under review for acceptance. It is placed in this chapter with the exact text in which it was submitted, with the formatting changed slightly to match the formatting of the thesis. This was done because the manuscript has not been accepted for publication as of the submission date of the thesis. An earlier version was submitted to the Transportation Research Board (TRB) for acceptance for publication, but was not accepted. This was beneficial to the manuscript as peer reviewed comments were returned with the article. These comments were reviewed and implemented into the paper to improve its clarity. The ACI Materials Journal is considered to be a better audience for the content of the manuscript and is more widely known throughout the world. It is anticipated that the manuscript will be accepted for publication as it has been peer reviewed and improved through the TRB comments.

Manuscript

Abstract

Concrete resistance to the penetration of chloride ions from deicing salts or brine solutions is an important performance indicator for mixture design specifications. The AASHTO T277 test can be used for approval of concrete mixture designs as an indicator of potential long-term behavior, but it is time consuming and not conducive to quality control or quality assurance (QC/QA) testing of field cured concrete. The Wenner probe device characterizes the electrical resistance of concrete, which has a role in both the initiation and propagation of corrosion. Fully developed life cycle analysis models use both of these components to address life expectancy. This paper demonstrates the connected physics relationship between these two tests. Using 26 different concrete mixture designs, the electrical resistivity is correlated with T277 results and predicts the resistance of concrete to the penetration of chloride ions with less effort and expense.

Introduction

Chloride-based deicing salts are commonly used on bridges and pavements during winter conditions to improve driving conditions and safety. The diffusion of dissolved chlorides through the concrete enhances the conditions for the steel reinforcement in bridge structures and continuously reinforced pavements to oxidize and subsequently corrode. The corroding steel eventually delaminates the concrete, resulting in the need to replace bridge decks, substructures, and pavements. Performance-based or high performance concrete specifications need measures that predict concretes which resist the intrusion of chloride ions. AASHTO T277 (T277)/ASTM C1202 (2,1) has been used to

predict concrete resistance to chloride ion penetration. This test is designed to verify mixture designs in a laboratory, but not for in-situ quality control measures. The T277 test requires a month or more of curing under controlled conditions and more than 24 hours to prepare and perform using vacuum saturation and 60Vdc impressed voltage to accelerate the chloride ingress. The test provides a relative measure of the resistance of concrete to the ingress of chloride ions, but not a measure of a fundamental material property of concrete.

A different approach of evaluating the resistance of concrete to transport chloride ions can make use of basic physics and material properties. A Wenner four probe device, by measuring the electrical resistivity of concrete using a fixed electrical current and voltage measurement, has been used to measure the properties of concrete for potential to allow for chloride ingress. This class of device reduces the time spent on sample preparation and testing. It also provides for a scientific measurement of properties that includes the effects of material quality, mixing, transportation, placement, and curing found in-situ, rather than laboratory preparation conditions.

Research Significance

Highway agencies and researchers could use the Wenner device to evaluate a performance measure of mixture designs and in-situ properties of constructed facilities, when a reliable correlation of these two testing methods existed or a range of application limitations existed. The durability of concrete structures could be determined more efficiently and in completed constructions. This could be used for quality assurance in concrete acceptance criteria.

Background

The AASHTO T277 method can be modeled as an electrical circuit composed of a power source and a resistor with a voltage drop across it, as seen in Fig. 4.1. The total charge in coulomb (amp-sec) passed is considered a relative measure of the resistance to chloride ingress of the concrete. In addition to time consuming preparation and testing time, the testing of the specimen can change the pore structure and resistivity of the specimen (6). The temperature rise in the cells over 6 hours results in a “joule effect” that eliminates the steady state condition of the test (12). Since low resistive concrete experiences a substantial temperature rise as compared to highly resistive concrete, the results are not linearly related but skewed.

The Wenner probe was originally designed to determine soil resistivity in soil strata, but has been adapted for concrete (4). A current is passed between the two outside contact probes, and the voltage drop between the two inner contact points is measured as shown in Fig. 4.2 (7). Results from using the Wenner device are in electrical resistivity ($k\Omega \cdot cm$). Research has been conducted to investigate the effects

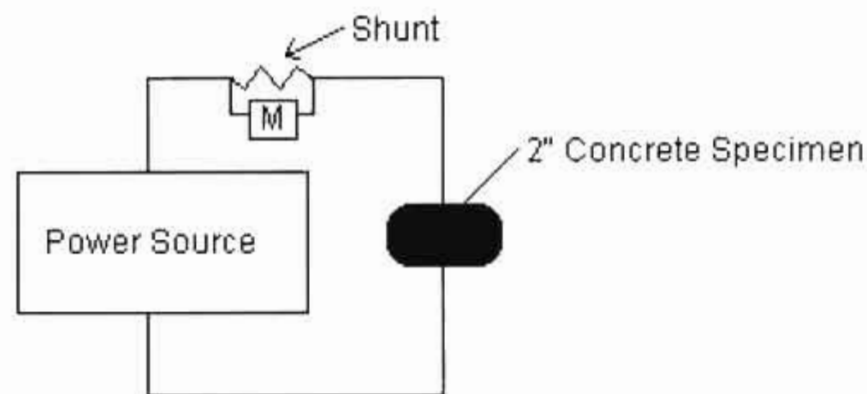


Fig. 4.1 – AASHTO T277 test apparatus

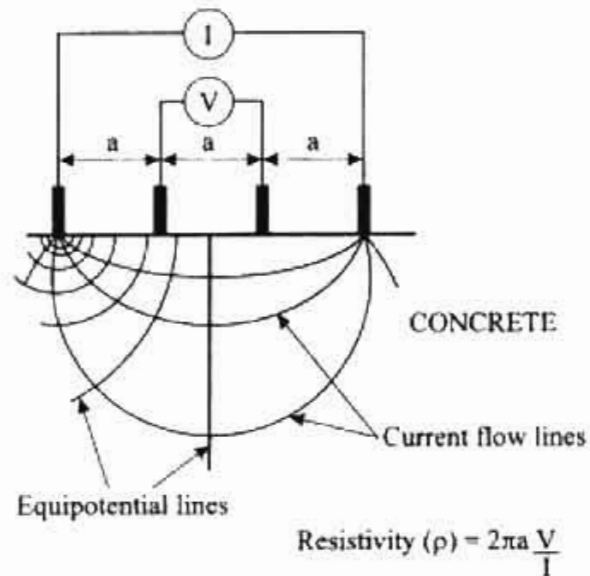


Fig. 4.2 – Wenner meter (7)

of probe spacing and other factors on resistivity readings (7,8,15,14). The Florida Department of Transportation has developed a method to standardize procedures for collection of resistivity readings (11).

Investigation into whether the AASHTO T277 testing method can accurately be used as a method of testing for chloride ion penetration was conducted by Feldman et al. (6). It was determined that the physical characteristics of the concrete specimens in the T277 test were changed by the high impressed voltage and vacuum saturation procedure found in the test, potentially leading to incorrect values. They determined that there was good correlation between current passed and conductivity (which is the inverse of resistivity). The data presented in this paper verifies their determination that there is a good correlation between current passed and conductivity through use of a Wenner device. Additional research was conducted to investigate all testing methods and the pros and cons of each method (15) as well as material influence on the T277 test (13).

Research was done on the effect of specimen geometry and probe spacing on resistivity readings by Morris et al. (9). This research was conducted to correlate readings from standard strength test cylinders with semi-infinite slabs in order to indirectly measure concrete characteristics. The experiment involved creating a finite element model of concrete specimens as well as testing specimens with a Wenner resistivity device. A correction factor was developed to correlate experimental and modeled values of resistivity with different probe spacing and specimen shape and size. This correction factor is called the geometric correction factor.

Experimentation using the Wenner device on 529 sample sets was conducted by Kessler et al. at the Florida Department of Transportation (10) to investigate whether resistivity can be used as a quality control measure in place of AASHTO T277. Their findings indicate that there is a good correlation between AASTHO T277 and resistivity with the application of the geometric correction factor.

The T277 test involves the application of 60Vdc, which increases the current flow producing excessive heating of the specimen and changing the pore structure of concrete over a short period of time. As a resistor (concrete specimen) is heated, the conductivity of the material increases. Since the AASHTO T277 is a measurement of conductivity in order to quantify chloride ion ingress, an excessive increase of specimen temperature during testing results in a higher T277 reading, created by the joule effect. A relationship between temperature change during testing and final coulomb readings was developed by Betancourt and Hooton (12) in order to eliminate excessive heating effects of the specimen during testing. These researchers also state that the joule effect has been a major obstacle in connecting T277 data and the electrical conductivity. They

recommended that research should be performed to validate the correlation in these two testing methods. The data presented in this paper shows the Wenner resistivity data and AASHTO T277 data are related with consideration of the joule effect.

The purpose of this work is to relate the AASHTO T277 testing results with results obtained using a Wenner resistivity device by Ohms law. It has been established that there is a correlation in the testing results based on experimental data. The idea that a connection exists using Ohms law has been presented (12), but no relationship has been developed. The main objective is to show that there is a scientific connection between the two testing results through Ohms law.

Experimental Investigation

Research has been conducted through a pooled-fund study (17) for the Federal Highway Administration (FHWA) on the durability of 26 different binary and ternary blends of cement. These blends of ASTM C150 Type II cement include pozzolans such as silica fume (SF), ground granulated blast furnace slag (GGBFS), two types of Class F fly ash (labeled F and F2), Class C fly ash, and metakaolin. In addition to different types of pozzolans, different types of cements were used including ASTM C595 Type IP (portland-pozzolan), and two Type IS (portland blast-furnace slag) cements, and an ASTM C1157 GU cement. These abbreviations are used next to percentages of each mineral admixtures for the remainder of this article (i.e., 75TI/20F2/5M indicates 75% Type I, 20% F2 fly ash, and 5% metakaolin). The water/cementitious materials ratio for these mixtures was 0.44. In order to meet the requirements of the study, an air-entraining

admixture and water reducer were used in all the mixtures. The aggregates used had a maximum nominal diameter of 19 mm (3/4 inch).

As part of this study, resistivity and AASHTO T277 readings have been obtained. To determine the relationship between the T277 test results and results obtained using the Wenner device, samples were prepared according to the T277 method and tested at 98-days (± 1 day). The specimens were tested at 98-days to capture the effects of the pozzolans that generally contribute to concrete resistivity after 28-days. The T277 specimens were wet cured in lime water for 14 days after being cast, then were dry cured under laboratory conditions until being tested. Specimen temperatures at the beginning of testing were kept constant between the two testing methods to avoid thermal interference outside of the joule effect.

Cylinders for resistivity measurements were cast and placed in a wet curing room in accordance with ASTM C192. They were removed from the plastic cylinders at 2 days and were wet cured until 98-day (± 1 day) readings were taken. An evaluation of the effect of saturation on resistivity readings was performed. Two cylinders from one mixture (65TI/30F/5SF) were left out and tested at 5 minutes, 35 minutes, and 55 minutes after being removed from wet cure with the results shown in Table 4.1. This was done to study the effects that standardization of testing would have on the resistivity readings.

Table 4.1 – Drying time effect on resistivity for 65TI/30F/5SF

Drying time (min)	Resistivity ($k\Omega \cdot cm$)	Difference vs. 5 min.
5	55.25	0%
35	63.25	14%
55	68.75	24%

Analytical Development

It is necessary to determine the resistivity from the AASHTO T277 data in order to compare with the results obtained using the Wenner device. These testing methods are related by Ohms law, shown in Equation (1), which relates voltage (V), current (I), and resistance (R) in an electrical circuit. To validate the Wenner device readings for concrete, data was collected experimentally in the lab and compared to the theoretical resistivity computed using the relationship in Equation (1) and AASHTO T277 readings.

$$I = \frac{V}{R} \quad (1)$$

The AASHTO T277 test can be modeled as an electrical circuit consisting of a power source, steady voltage drop, and a resistor. The basic equation for electrical resistivity is Equation (2) and is calculated by rearranging the Ohms law equation in Equation (1). The resistivity (ρ) of the specimen used in T277 can be determined using Equation (3) by substituting the resistance into Equation (2). The units of resistivity are expressed as $k\Omega \cdot \text{cm}$ ($k\Omega \cdot \text{in}$). The T277 test has a constant voltage drop (60 Vdc) across the resistor, a measured current value and time interval, and the dimensions of the specimen are also known, so resistivity can be directly calculated. In this way, the data from the AASHTO T277 method can be theoretically compared to data obtained using the Wenner device.

$$\rho = R * \frac{\text{Area}}{\text{Thickness}} \quad (2)$$

$$\rho = \frac{V \times Area}{I \times Thickness} \quad (3)$$

The converted coulomb value was then calculated using Equation (3) and the experimental resistivity data collected using the Wenner device. In Equation (3), coulombs were determined by solving for the current (I), then multiplying the current value by the T277 testing time (6 hours = 21,600 seconds). The resulting value is the theoretical coulomb value calculated using the Wenner resistivity device readings.

The Wenner technique uses a series of four probes connected to a power source. The spacing of the probes is constant ($a=5.1$ cm [2 inches]), a known current is passed between the two outer probes, and the resulting voltage drop across the two inner probes is measured. A diagram of this arrangement is shown in Fig. 4.2. The equation for determining the resistivity using the Wenner device is shown in Equation (4),

$$\rho = 2 * \pi * a * \frac{V}{I} \quad (4)$$

where “ a ” is the distance between probes.

Current is not one dimensional; it is a three-dimensional field. When resistivity is measured on a round cylinder using the Wenner meter, the current is restrained within the concrete and interference is caused by the concrete and air interface. Resistivity readings from a semi-infinite flat slab represent the standard for resistivity of the material, whereas the resistivity from the curved cylinder has interference from the edge of the cylinder. In order to account for this interference, the data needed to be converted into an equivalent

semi-infinite slab resistivity where there are no curvature effects. This was accomplished with a geometric correction factor (K). This correction factor was first established by Morris et al. (9) and was verified by independent testing for 10 cm by 20 cm (4 inch x 8 inch) cylinders for this study. The values obtained by using the Wenner device should be divided by the proper correction factor as in Equation (5) (9), which was determined to be $K = 2.7$ for 5.1 cm (2 inch) probe spacing and 10 cm by 20 cm (4 inch x 8 inch) cylinder. This correction factor was used to determine the adjusted resistivity reading values shown in Table 4.2. The geometric correction factor is applied equally to all 10 cm by 20 cm (4 inch x 8 inch) cylinders used in this test. The Florida Department of Transportation (13) used this to develop the limits for the FDOT resistivity testing method (11).

$$\rho_{\text{real}} = \rho_{\text{measured}} / K \quad (5)$$

The joule effect was considered to account for heating of the specimens during AASHTO T277 testing. This heating of the specimens may result in incorrect permeability results. A relationship was developed by Betancourt and Hooton (12) to account for specimen heating during testing. The equation developed is Equation (6), where Q_o is the total corrected charge, $Q_{c,6h}$ is the measured charge obtained from AASHTO T277 corrected for specimen diameter, β is an experimental constant equal to 1245, and δT is the temperature rise during testing (in Kelvin). The results of using Equation (6) are different for every mixture and vary depending on the amount of joule

Table 4.2 – Wenner resistivity conversions to coulomb

Mixture	Wenner Method			
	Measured Resistivity (ρ)	Geometric K Factor	Geometric Adjusted Resistivity (GAR)	Calculated Coulombs from GAR
	$k\Omega \cdot \text{cm}$ ($k\Omega \cdot \text{in}$)		$k\Omega \cdot \text{cm}$ ($k\Omega \cdot \text{in}$)	Coulombs
75TI/20F/5M	28.7 (11.3)	2.7	10.6 (4.2)	1711
60TI/30F/10F2	8.4 (3.3)	2.7	3.1 (1.2)	5857
60TI/20F2/20G120S	42.4 (16.7)	2.7	15.7 (6.2)	1158
75TI/20F2/5M	42.6 (16.8)	2.7	15.8 (6.2)	1152
67TI/30F2/3SF	36.3 (14.3)	2.7	13.4 (5.3)	1352
60TI/20F/20F2	14.8 (5.8)	2.7	5.5 (2.2)	3328
100TIP	20.5 (8.1)	2.7	7.6 (3.0)	2394
60TI/30F2/10C	17.0 (6.7)	2.7	6.3 (2.5)	2887
75TISM/25C	18.7 (7.3)	2.7	6.9 (2.7)	2630
75TISM/25F2	30.6 (12.1)	2.7	11.3 (4.5)	1603
97TISM/3SF	49.3 (19.4)	2.7	18.2 (7.2)	997
75TI/20F/5SF	36.4 (14.3)	2.7	13.5 (5.3)	1349
100TI	17.9 (7.0)	2.7	6.6 (2.6)	2746
65TI/30F2/5SF	64.0 (25.2)	2.7	23.7 (9.3)	767
65TIP/35G120S	73.8 (29.0)	2.7	27.3 (10.8)	666
60TI/20F/20G120S	36.3 (14.3)	2.7	13.4 (5.3)	1354
100E	16.7 (6.6)	2.7	6.2 (2.4)	2938
80E/20G120S	29.8 (11.7)	2.7	11.0 (4.3)	1650
95E5SF	46.0 (18.1)	2.7	17.0 (6.7)	1068
62TI/35G120S/3SF	62.8 (24.7)	2.7	23.3 (9.2)	782
60TI/35G120S/5M	65.1 (25.6)	2.7	24.1 (9.5)	754
75TI/20F2/5SF	65.6 (25.8)	2.7	24.3 (9.6)	748
77TI/20F2/3SF	42.4 (16.7)	2.7	15.7 (6.2)	1158
65TISM/35G120S	39.2 (15.4)	2.7	14.5 (5.7)	1253
50TI/35G120S/15SF	47.2 (18.6)	2.7	17.5 (6.9)	1040
85TIP/15F	25.8 (10.2)	2.7	9.6 (3.8)	1902

Note: 75TI/20F/5M = 75% Type I cement, 20% Class F fly ash, 5% metakaolin

effect adjustment required. For mixtures with higher permeability (higher coulomb, lower resistivity), larger heating variations occur during testing as compared with low permeability mixtures. This is due to larger currents passing through the interconnected voids. For these permeable mixtures, larger temperature variations produce larger joule effect adjustments. The joule effect adjustment was used to determine the adjusted T277 coulomb values shown in Table 4.3.

$$Q_o = e^{[\ln(Q_{c,6h}) + \beta(1/\delta T - 1/273)]} \quad (6)$$

A relationship may be established by comparing values determined from the same concrete mixture using the AASHTO T277 method with Equation (3) and the Wenner Technique with Equation (4). However, these relationships must be normalized to a uniform ambient condition. With the application of both the geometric correction and the adjustment for the joule effect, the results can be analytically combined as an evaluation tool for concrete. The results can be completed quickly and with less effort using the Wenner device to determine the chloride ion ingress into concrete. The testing procedure using the Wenner device requires approximately 30 minutes for completion, as compared to over 24 hours for the AASHTO T277 method. A comparison of the two testing methods is presented in Fig. 4.3 through Fig. 4.9 for both corrected and uncorrected resistivity.

Table 4.3 – AASHTO T277 conversions to resistivity

Mixture	AASHTO T277		
	Raw Average T277 Data	Joule Effect Adjusted T277	Calculated Resistivity from T277 (ρ)
	Coulomb	Coulomb	$k\Omega \cdot \text{cm}$ ($k\Omega \cdot \text{in}$)
75TI/20F/5M	1621	1369	13.3 (5.2)
60TI/30F/10F2	6786	3871	4.7 (1.8)
60TI/20F2/20G120S	2316	1804	10.1 (4.0)
75TI/20F2/5M	2363	1877	9.7 (3.8)
67TI/30F2/3SF	1987	1611	11.3 (4.4)
60TI/20F/20F2	5490	3431	5.3 (2.1)
100TIP	4023	2715	6.7 (2.6)
60TI/30F2/10C	6137	3558	5.1 (2.0)
75TISM/25C	4023	2725	6.7 (2.6)
75TISM/25F2	3032	2173	8.4 (3.3)
97TISM/3SF	935	845	21.5 (8.5)
75TI/20F/5SF	1163	1032	17.6 (6.9)
100TI	4562	3068	5.9 (2.3)
65TI/30F2/5SF	1512	1308	13.9 (5.5)
65TIP/35G120S	1176	1040	17.5 (6.9)
60TI/20F/20G120S	2000	1709	10.6 (4.2)
100E	5890	3649	5.0 (2.0)
80E/20G120S	1970	1703	10.7 (4.2)
95E5SF	1656	1415	12.9 (5.1)
62TI/35G120S/3SF	984	872	20.9 (8.2)
60TI/35G120S/5M	698	627	29.0 (11.4)
75TI/20F2/5SF	1230	1071	17.0 (6.7)
77TI/20F2/3SF	1900	1555	11.7 (4.6)
65TISM/35G120S	1568	1318	13.8 (5.4)
50TI/35G120S/15SF	1437	1216	15.0 (5.9)
85TIP/15F	3634	2555	7.1 (2.8)

Note: 75TI/20F/5M = 75% Type I cement, 20% Class F fly ash, 5% metakaolin

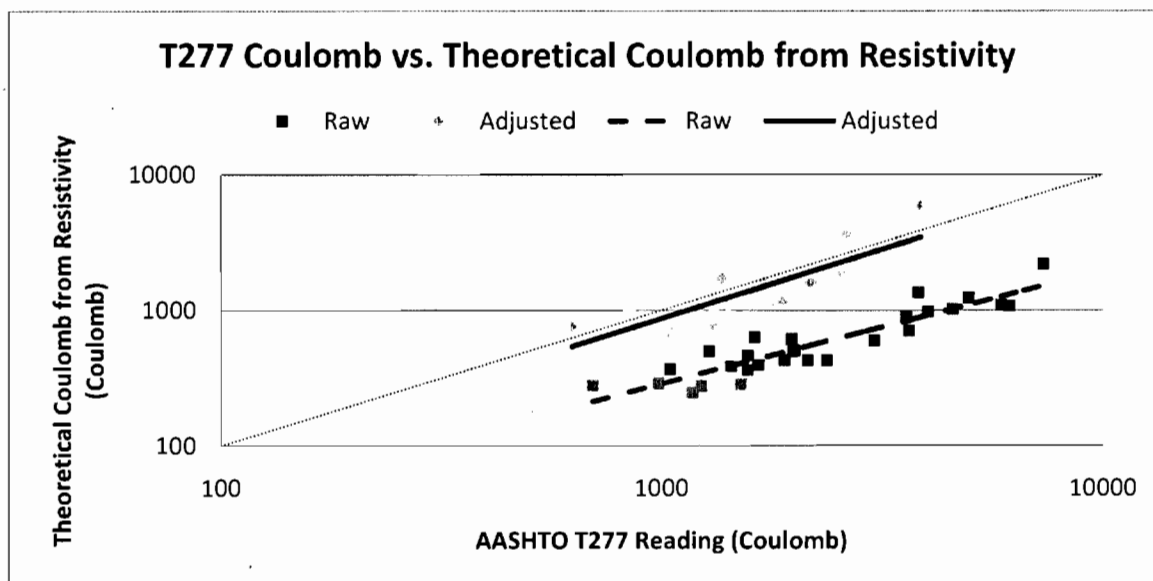


Fig. 4.3 – Raw coulomb and adjusted coulomb (joule effect and geometric correction)

Results

Resistivity and AASHTO T277

In order to verify a relationship using Ohms law, three different ways of analyzing the data needed to be investigated. The first type of analysis done was to calculate equivalent coulomb values from resistivity data and compare it to the T277 coulomb data. The second method was to calculate equivalent resistivity from T277 data to compare with the Wenner resistivity data. The third type of analysis done was to compare T277 coulomb data and Wenner resistivity data.

To develop a relationship between the AASHTO T277 test and resistivity, data was collected and shown in Fig. 4.3 through Fig. 4.9. Each data point represents average values of resistivity with 8 readings per cylinder and an average of 2 cylinders per

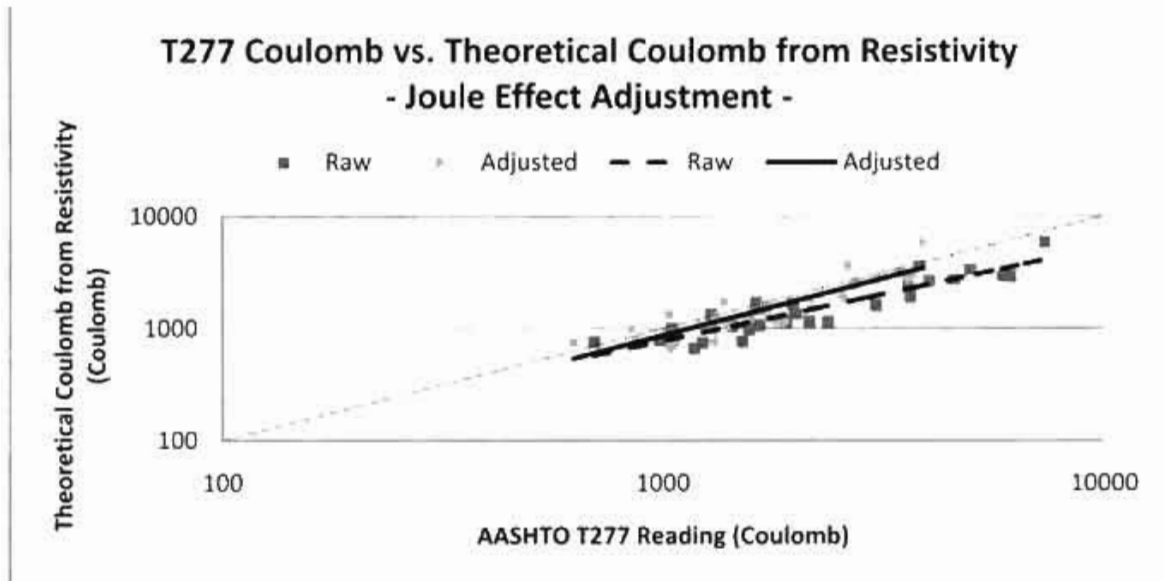


Fig. 4.4 – Raw coulomb and adjusted T277 coulomb (joule effect)

mixture, and 2 to 6 specimens for AASHTO T277. By comparing coulomb values from T277 with calculated coulomb from resistivity as in Fig. 4.3 through Fig. 4.5 and Table 4.2, it can be seen that there is a strong need for using the joule effect adjustment and geometric correction factor to relate these two testing methods through Ohms law. The closer the line is to a 1:1 relationship, the better the relationship is between these two methods using Ohms law. Fig. 4.3 shows the adjusted (including joule effect and geometric correction factor) and raw (no adjustment) coulomb relationship. The correlation is near the 1:1 relationship with the adjustments. To understand how each of these corrections affects the data, they are plotted separately in Fig. 4.4 and Fig. 4.5, keeping the joule effect adjustment or geometric correction unchanged for each plot. The trend in Fig. 4.4 is due to the excessive heating of the specimens caused by high permeability mixtures. As can be seen, both adjustments are made to account for most of the differences in the coulomb relationship for Ohms law for these two testing methods.

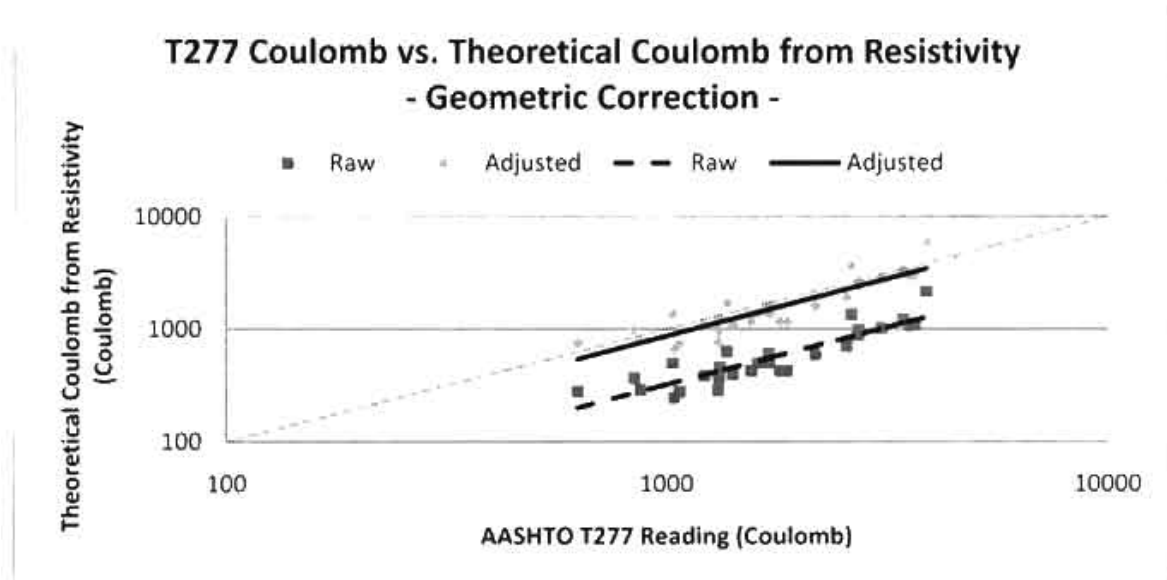


Fig. 4.5 – Raw coulomb and adjusted (geometric correction) coulomb obtained from resistivity (Wenner meter)

The same trend is observed as in the coulomb comparisons for calculated resistivity in Fig. 4.6 through Fig. 4.8 and Table 4.3. Similar to the coulomb comparisons, either the joule effect adjusted values or the geometric corrected values are kept the same for each plot to observe the effect of the adjustment. With the adjustments, it is observed that the relationship is much closer to a 1:1 relationship than without these corrections. Two sets of data are presented in Fig. 4.7 with the geometrically adjusted resistivity remaining unchanged, one showing the T277 raw data converted to resistivity and the other showing the joule effect factored into the calculations for T277 data. With the joule effect adjustment, the relationship between the calculated resistivity from T277 and the experimentally determined resistivity is closer to a 1:1 relationship, as would be expected with Ohms law. Fig. 4.8 shows the effects of varying the geometric correction

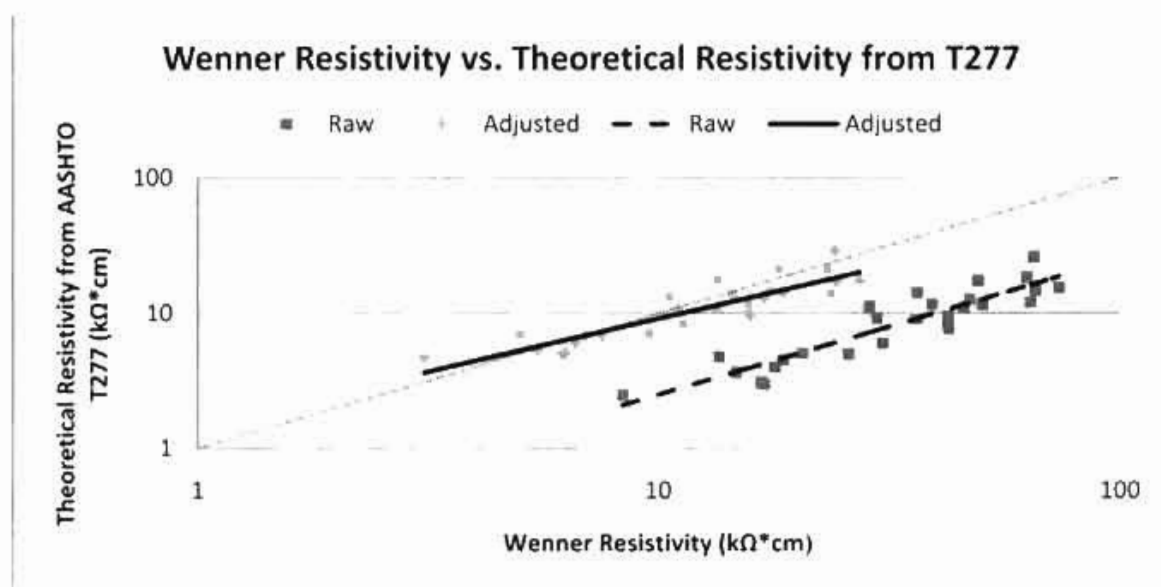


Fig. 4.6 – Raw resistivity and adjusted resistivity (joule effect and geometric correction) ($l=2.54\text{cm}$)

factor while keeping the adjusted T277 data unchanged. Again, with this correction the relationship is much closer to unity than before the correction. It has been observed that there is a change in slope between the joule effect adjusted values and the raw data values. The main reason for this change in slope is due to heating of the test system through permeable mixtures and, therefore, more adjustment is required.

In Fig. 4.9, a theoretical line is presented that represents coulomb values based on T277 testing in correlation with resistivity calculated from the T277 results along with the raw data for comparison. There is a relationship between AASHTO T277 and resistivity readings based on the fit of the trend line to the data and the proximity of the trendline to the theoretical line.

By using the theoretical adjustments for the joule effect and the geometric correction factor, it can be seen that the adjusted predictive line in Fig. 4.9 is much closer

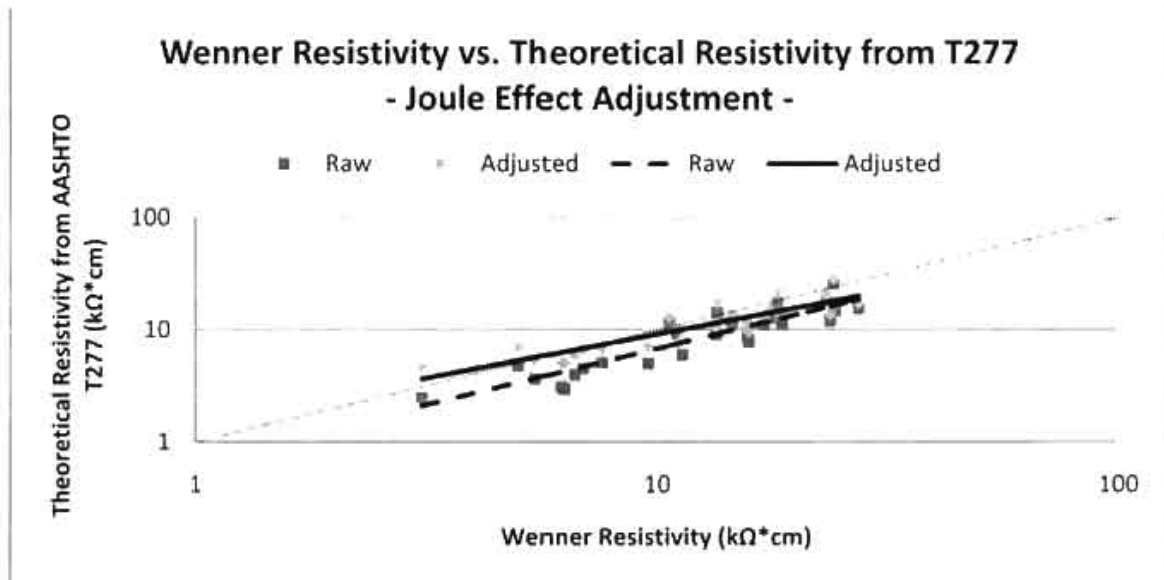


Fig. 4.7 – Adjusted resistivity (joule effect) calculated from T277 data (lin=2.54cm)

to the theoretical values obtained from AASHTO T277. There still exists a variance between the theoretical and adjusted values; however, this can be explained by looking at surface resistivity vs. concrete resistivity. Surface resistivity is determined by the Wenner device and only determines the resistivity a small distance into the concrete (up to a depth equal to the probe spacing). Concrete conductivity is determined through the AASHTO T277 test over the entire depth of the specimen. The difference between the theoretical and empirical readings is due to the presence of more paste at the surface of the concrete, which has a different resistivity than the center of the concrete where less paste exists.

Variation in Relationship

To understand how closely the adjusted equation shown in Fig. 4.9 is to the theoretical equation, an investigation into the percent variation between the results of

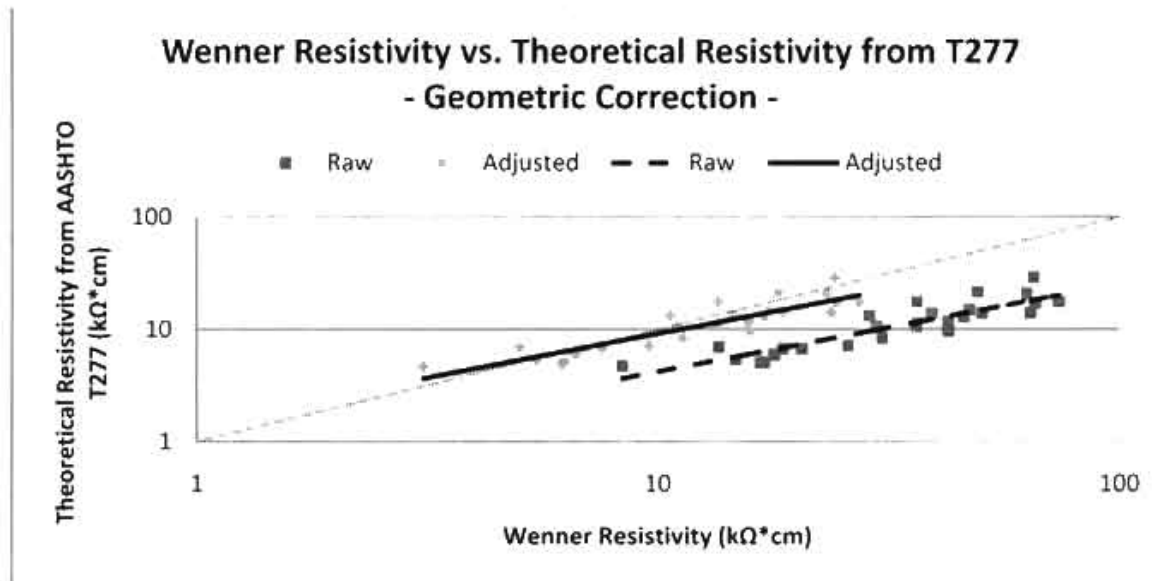


Fig. 4.8 – Raw resistivity and adjusted (geometric correction) Wenner resistivity
($l = 2.54\text{cm}$)

each equation was performed. Fig. 4.10 shows the same equations and relationship as Fig. 4.9, but with the variation limits shown in a variation triangle. The top of the triangle shows where there is no variation (where the two equations are equal) and the first row from the top shows where the results of each equation vary by approximately 5% (to the right of the vertical line, the adjusted equation overestimates the coulomb value by 5% and to the left it underestimates by 5% from the theoretical value). Larger variations are observed in dense, low permeable concrete, but smaller with higher permeable concrete. This provides greater confidence in values of greatest concern.

Summary and Conclusions

In order to use chloride ion penetration as part of a durability acceptance criterion, an effective and simpler means of testing concrete other than the AASHTO T277 test

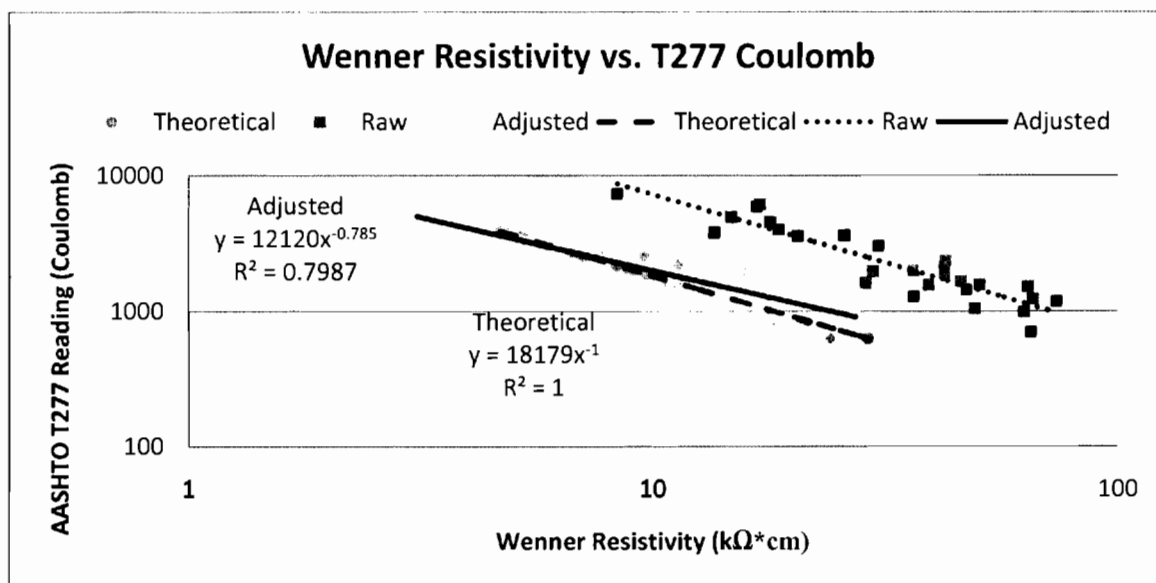


Fig. 4.9 – Wenner resistivity vs. AASHTO T277 coulomb (1 in=2.54cm)

needs to be used. Through this research and work performed by other researchers, it has been observed that there is a correlation between AASHTO T277 and resistivity using a Wenner four probe device. The AASHTO T277 6-hour testing results and results obtained using a Wenner resistivity meter can be related through Ohms law for blended and unblended cement concrete mixtures. This is particularly true for mixtures with higher permeability.

Through the results of this research, it is possible to obtain resistivity measurements from a 10 cm by 20 cm (4 inch by 8 inch) cylinder and compare them to theoretical resistivity data obtained by using AASHTO T277. This can be done by using adjustments for cylinder geometry for resistivity and the joule effect during testing for T277. These adjustment factors were verified through independent testing. It is possible to obtain correlations for ternary mixture, binary mixture, and unblended cement concretes through the use of these factors.

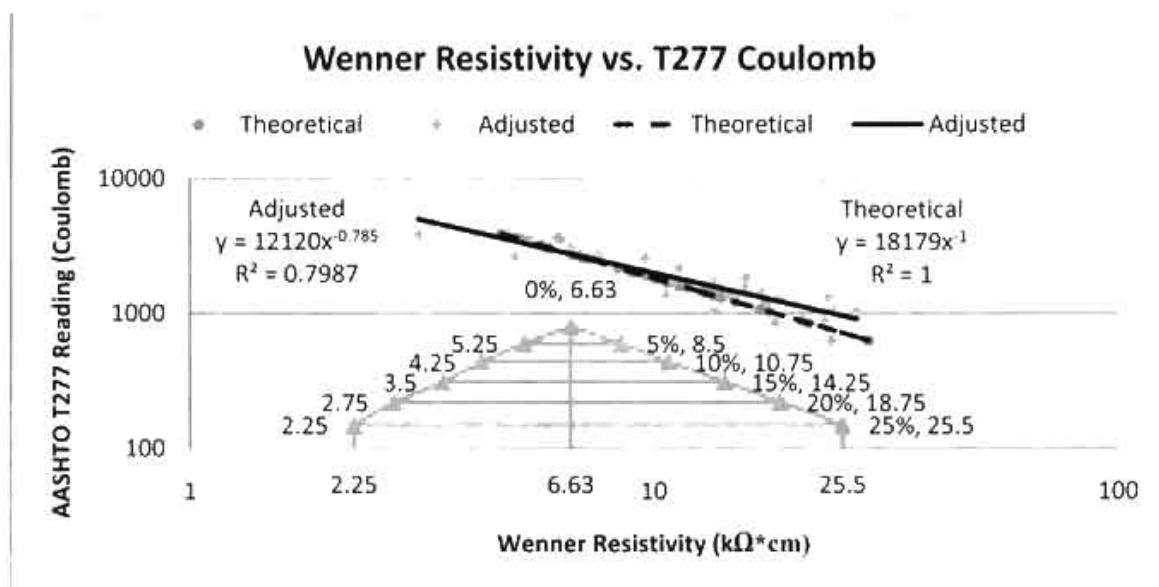


Fig. 4.10 – Comparison of adjusted (joule effect and geometric correction) relationship and theoretical relationship ($l=2.54\text{cm}$)

This data supports the use of the Wenner device as a quality assurance/quality control (QA/QC) tool in concrete field testing. A testing method needs to be developed that specifies the dry curing period between wet curing and time of testing in order to standardize and compare the results. Continued research on how to ensure that in-situ concrete is saturated to an acceptable level (saturated surface dry) should be performed in addition to environmental effects on in-situ resistivity readings. Cylinders cast as QA specimens and placed in wet curing for strength testing could be used for resistivity testing.

CHAPTER 5

EVALUATION OF DATA

This chapter provides further explanation for the results portion of the ACI manuscript found in Chapter 4 as well as other information not included in the manuscript.

Geometric Correction

The curvature of the concrete specimen introduces distortions in the electrical field that affect the resistivity value measured by the Wenner device. The Wenner probe passes a current between the two outside probes, and the voltage drop across the inner probes is measured. As the current is three-dimensional, it reaches the boundary between the curved surface of the cylinder and the air at various angles to the direction of the probes. This causes the current to be concentrated within the conducting material and so larger values of voltage are measured as compared to a semi-infinite flat slab. The correction factor for the 4 inch by 8 in cylinder was tested for validity for the ACI manuscript in Chapter 4. This testing involved six 4 inch by 8 inch cylinders and one 1 foot by 1 foot by 4 inch slab. The readings were taken diagonally on the slab to minimize edge interference. As can be seen in Table 5.1, using a correction factor of 2.7, the

Table 5.1 – Independent testing of geometric correction factor

Specimen Shape	Avg. reading 28 day	Geometric Correction	Adjusted Resistivity	Difference (%)
1 ft x 1 ft x 5 in Slab	22.4 k Ω *cm	1	22.4 k Ω *cm	5.5%
4 in x 8 in Cylinder	57.0 k Ω *cm	2.7	21.1 k Ω *cm	

4 inch by 8 inch cylinder results were very close to the results obtained for a flat slab. The effect of this correction can be seen in Fig. 4.5 in which the geometric correction factor corrects the Wenner resistivity data (used to determine coulomb in Fig. 4.5) closer to an Ohms law relationship. The one-to-one relationship is considered an Ohms law relationship due to both methods yielding the same result, shown as the diagonal line.

The geometric correction factor also includes the differences in surface resistivity of the specimens as well. There may be a difference in surface resistivity between the vertical cylinder and horizontal slab as the horizontal slab may have more paste at the surface than the edge of the cylinder. This is discussed more in the suggested additional research section at the end of this chapter.

Joule Effect

The joule effect correction was applied to the ASTM C1202 data after testing. This correction was done to account for the effects of heating of the specimen during testing. As stated earlier, as the temperature of the specimen increases, so does the electrical conductivity. As the ASTM C1202 test is a measurement of conductivity through the specimen, it was expected that as the temperature would rise, so would the current passed. In order to test this expectation, specimens were cast and prepared the same as with all other testing done for this thesis. The specimens chosen were at both

ends of the permeability spectrum, that is, high permeability and low permeability. One set of these specimens were tested for a longer duration (36 hours) with lower applied voltage (10V); the others were tested using the ASTM C1202 method (60V over 6 hours) with the joule effect adjustment applied using Equation (4). In this way, the same energy was applied to the cell prolonged over an extended period of time as was applied during the normal testing time. This was expected to cause less temperature rise during testing and allowed for direct comparison with the temperature corrected specimens. It was found that the results comparing the temperature corrected specimen data and the prolonged testing time were very close for the higher permeable mixtures and not quite as close for lower permeable mixtures, as can be seen in Table 5.2. The standard deviation for these specimens was 646 coulombs, the mean was 1129, and the coefficient of variation was 0.57, which was considered acceptable. Fig. 5.1 shows both the temperature rise and current increase over the testing period for both the extended testing time and the standard testing time (6 hours). The area between the standard testing time and the extended testing time is the joule effect. It was concluded that the joule effect must be considered when performing the ASTM

Table 5.2 – Extended testing coulomb vs. joule corrected coulomb

Mixture	Specimen	Normal ASTM C1202 Test			Extended	Variation
		Initial Temp (c)	Final Temp (c)	Joule Corrected Coulomb	Extended Test Coulomb	Percent Different
75TI/20F2/5M	1	21	32	1,268	1,072	18%
	2	21	32	1,359	1,008	35%
62TI/35G120S/3SF	1	21	28	888	737	20%
	2	22	30	855	761	12%
60TI/35G120S/5M	1	21	27	921	545	69%
	2	20	27	683	602	13%
100TI	1	21	45	2,555	2,552	<1%

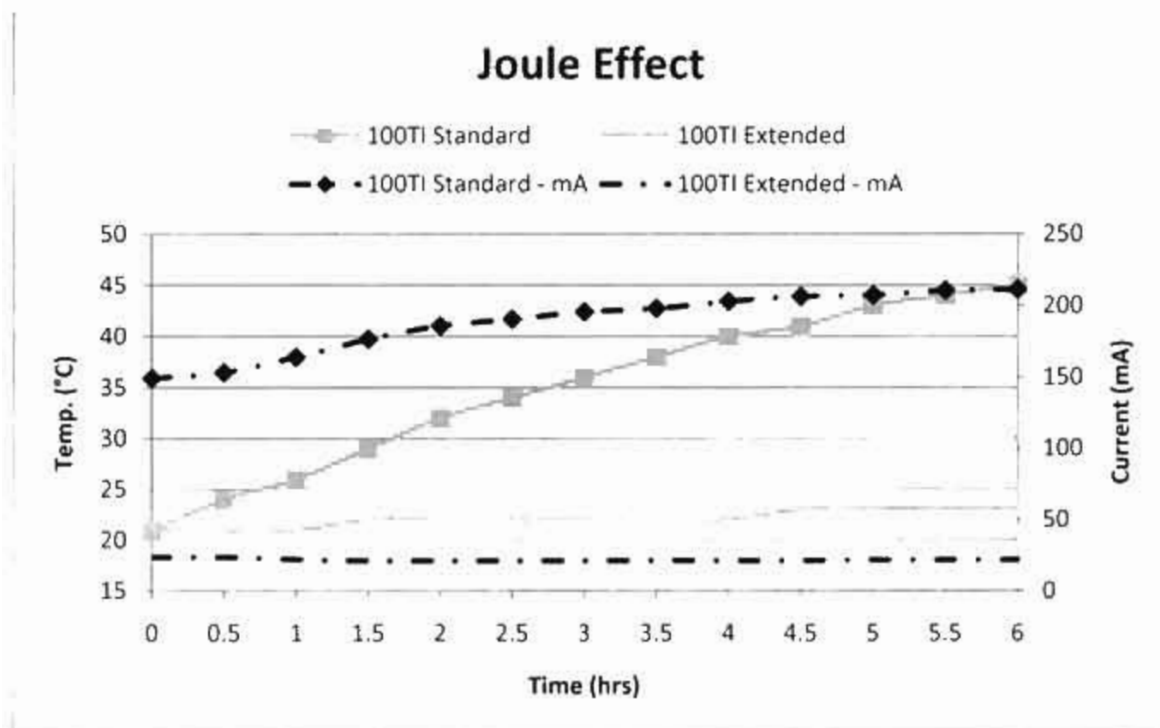


Fig. 5.1—Joule effect

C1202 test in order to get more realistic information about the material properties without the interference of specimen heating. The effect of this correction can be seen in Fig. 4.4 in which it corrects the ASTM C1202 data closer to an Ohms law relationship. The one-to-one relationship is considered an Ohms law relationship due to both methods yielding the same result.

Resistivity from Coulomb and Coulomb from Resistivity

Resistivity from Coulomb

In order to understand the relationship between the ASTM C1202 testing method and Wenner resistivity, it was important to calculate resistivity from the ASTM C1202 data using Ohms law and compare the results with experimental resistivity using the

same concrete. In order to determine the equation needed to convert the ASTM C1202 data into resistivity, certain basic principles need to be understood.

Ohms law states that current flowing in a material is directly proportional to the potential difference across the ends of a resistor divided by the electrical resistance.

Another basic concept is the resistivity of a material, which is how strongly a material opposes the flow of electric current. A low resistivity means that the current can flow through the material with ease; conversely, the higher the resistivity, the more opposition the current experiences through the material. Resistivity is the resistance of the material multiplied by the cross-sectional area of the material divided by the length of material (see Equation (3)). Combining Ohms law with resistivity by inputting the equation for Ohms law into the resistivity equation allows the resistivity of a material to be determined (see Equation (4)). The required information is the potential voltage drop across the material, current applied to the material, cross sectional area, and thickness of the material, all of which are known or can be derived from the ASTM C1202 results.

By taking the Coulomb (Amp*sec) value corrected for the joule effect from ASTM C1202, which has a nearly constant current applied, and dividing it by the total time of the test (6 hours = 21,600 seconds) it was possible to determine the average current applied during testing. Then taking the constant potential applied during testing (60V), multiplying it by the cross sectional area of the concrete specimen (using a diameter of 3.75 inches as stated in Chapter 3), dividing it by the average current and thickness of the specimen, the resistivity was obtained. The results of this can be found in Table 4.1.

Coulomb from Resistivity

Another method to check if an Ohms law relationship existed between the ASTM C1202 testing method and Wenner resistivity was to convert geometrically corrected resistivity into coulomb using Ohms law. By following the methodology in the previous section, solving for current instead of solving for resistivity, the coulomb values could be determined using Ohms law. If the potential difference is assumed to be the same as is used in ASTM C1202 (60V) and all the other parameters are known, Equation (4) could be rearranged and the current could be solved for. Once the average current is solved and multiplying it by the testing time, coulombs are determined. A summary of selected mixtures is given in Table 4.2.

Deviation from Theoretical Ohms Law

As is generally the case between theoretical equations/relationships and experimental data in concrete, there is a variation between the theoretical Ohms law relationship between these tests and the experimental. This is evident in Fig. 4.10. The variation is greater with low permeability mixtures than for higher permeability mixtures, and the relationship is equal at $6.63 \text{ k}\Omega \cdot \text{cm}$. One reason for this variation may be that the geometric correction factor, as stated above, may not be the same for low permeable mixtures as it is with high permeable mixtures. The triangle shape in Fig. 4.10 shows the variation at different resistivity values between the theoretical line and the adjusted line. These were determined by using the same resistivity value in each equation and comparing the results. Table 5.3 shows the results of each equation and the variation at

Table 5.3—Adjusted equation variation from theoretical equation

Resistivity k Ω *cm (k Ω *in)	Theoretical Eqn. (coulomb)	Adjusted Eqn. (coulomb)	% Variation
6.57 (2.6)	2768	2768	0%
8.5 (3.3)	2139	2261	5%
10.75 (4.2)	1691	1881	10%
14.25 (5.6)	1276	1508	15%
18.75 (7.4)	970	1216	20%
25.5 (10)	713	956	25%

each point to the right of equality. This comparison is done to show how closely the theoretical trendline and the experimental data trendline are.

Drying Time and Excluded Data

Some of the testing data was excluded from the presented results as a result of incorrect or inconsistent testing methods. Two sets of ASTM C1202 data were excluded due to a large difference in testing results. It was not desirable to include some of the data from the sets and not others. Resistivity data were also excluded due to improper curing before testing. The specimens were left out to dry longer than the 15 minute window used for this test, yielding higher resistivity values from poor contact areas.

Through testing the effects of drying time, it was determined that the longer the specimens were left out, the higher the resistivity. Table 4.3 shows the duration of time left out to dry and the resistivity reading obtained using a mixture with a moderate coulomb value.

Comparison with Prior Work

Burke and Hicks (16) developed a relationship between the ASTM C1202 and electrochemically determined resistivity. This relationship is shown in Fig. 5.2 along with the adjusted and theoretical relationships developed in Chapter 4. As can be seen, all the relationships are in a similar range and are relatively close to each other. It is important to note that the Burke relationship does not extend beyond 2,000 coulombs, because the information was determined to be inaccurate due to heating of the specimens, or what we now know as the joule effect. The difference in the lines is possibly due to variability in the geometric effect for lower permeable mixtures.

Material Influence Evaluation

Effects on Resistivity

Resistivity testing was performed at the University of Utah as part of the pool funded study on 27 of the 48 mixtures studied. Eleven more were completed, but due to saturation variations, the data were shown not to be reliable. An additional 7 did not have enough materials to complete.

The relationship between ASTM C1202 and Wenner resistivity can be seen in Fig. 5.3; the theoretical trend line is shown for resistivity values calculated using Ohms law and ASTM C1202 data from all samples. To understand the chart, a higher coulomb value (lower the resistivity) indicates the mixture is less resistant to chloride ion penetration. Fig. 5.3 (similar to Fig. 4.9) shows the inverse relationship between coulomb and resistivity, where when coulomb is high, resistivity is low. As ASTM C1202 measures the conductivity of the material and resistivity measures the

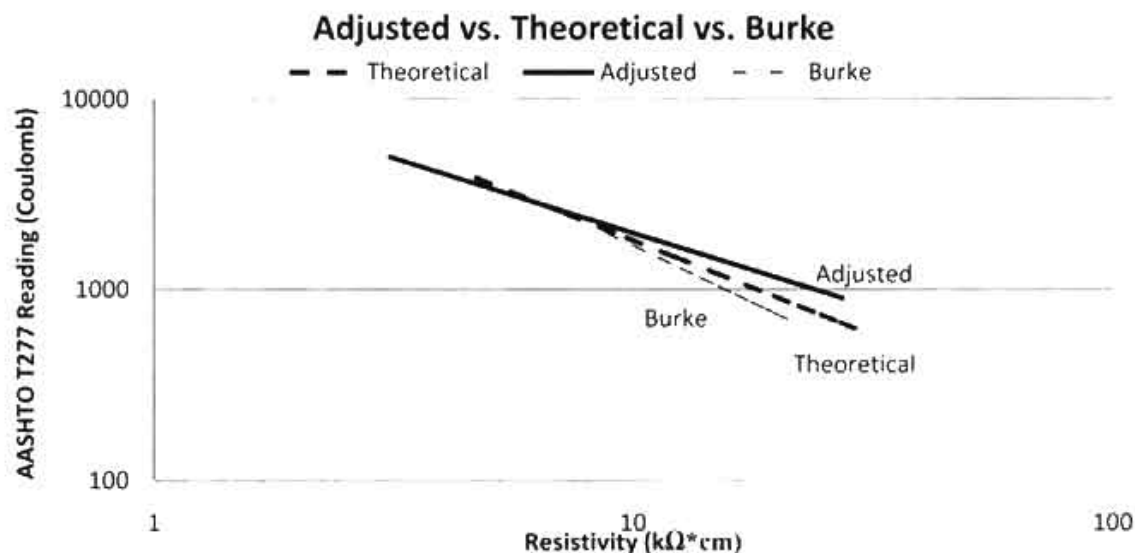


Fig. 5.2—Comparison to previous work

resistance of the material, it is expected that there is a relationship between the two because conductance is the inverse of resistance.

Each marker in Fig. 5.3 represents a different mixture and includes 8 to 48 resistivity readings using a Wenner device that were then averaged to obtain the data point. These mixtures were made of ternary cements, binary cements, and single cement mixtures and were cured for 98 ± 1 day. This testing time was chosen to ensure the majority of the pozzolans reacted in the concrete. We believe that through additional testing, the correlation of these two methods would improve.

Material Substitution Observations

Mixtures containing any ternary combination of Class F, C, F2 fly ashes had T277 performance levels higher than the control of 100% Type I/II. High volumes of fly ash generally increase the bleed water, which led to an increase in T277 values as

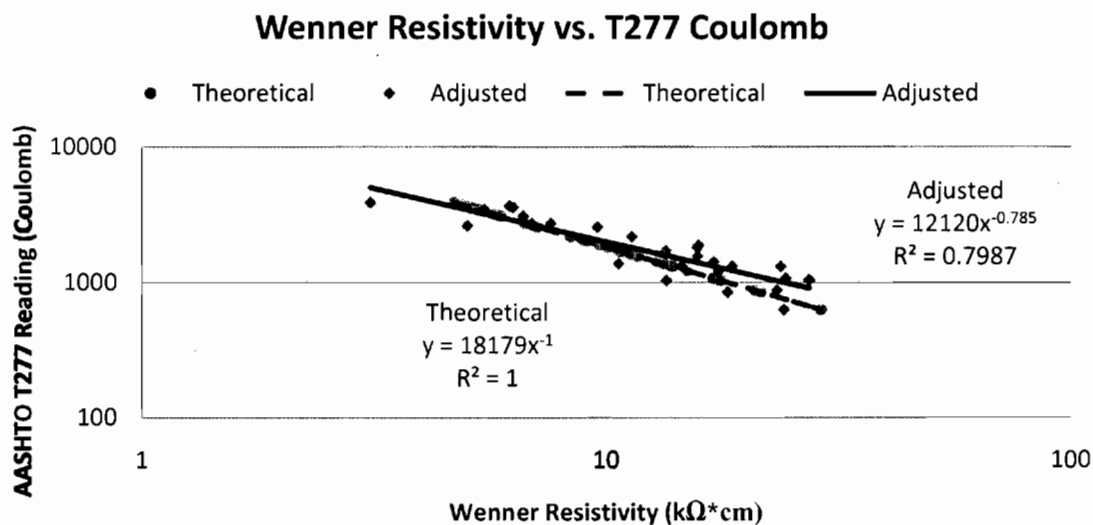


Fig. 5.3—AASHTO T277 coulomb vs. Wenner resistivity

interconnected voids appear in the mixtures. When larger amounts of fly ashes are combined, it increases the amount of bleeding as the spherical shape of the fly ash particles does not interact with water as other pozzolans do, such as silica fume. A decrease in water to cementitious material may be warranted in these mixtures.

It was observed in Fig. 5.4 that with Type I/II cement and a replacement of 40% cementitious material with 30% Class F2 fly ash and 10% Class C fly ash that a coulomb reading of 6137 and a resistivity reading of 17 $k\Omega \cdot cm$ (6.7 $k\Omega \cdot in$) were obtained. By replacing only 33% of cementitious material with 30% Class F2 fly ash and 3% silica fume, a coulomb reading of 1988 and resistivity reading of 36.313 $k\Omega \cdot cm$ were obtained. This substitution produced a reduction of 67.6% for coulomb and an increase of 113% for resistivity. Similarly, with Type I/II cement and a replacement of 40% cementitious material with 20% Class F fly ash and 20% Class F2 fly ash, readings of 4963 coulombs and 14.75 $k\Omega \cdot cm$ (5.8 $k\Omega \cdot in$) were obtained. By replacing the 20% Class F fly ash with

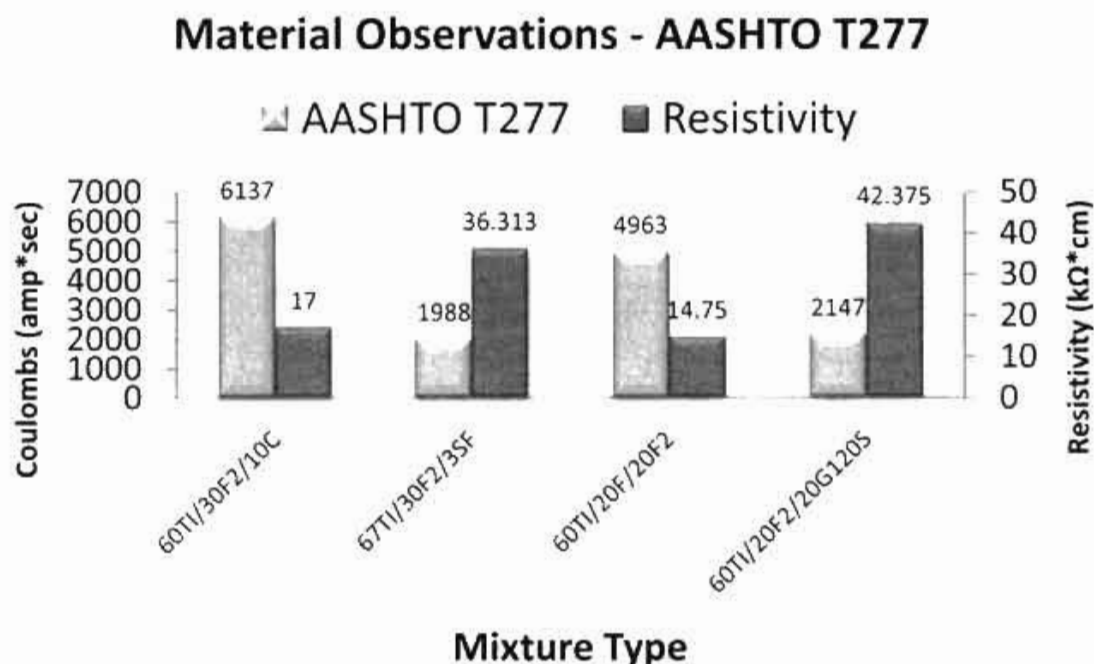


Fig. 5.4—Pozzolan substitution comparison (1 in=2.54cm)

20% G120 ground granulated blast furnace slag, readings of 2147 coulomb and 42.375 kΩ*cm (16.7 kΩ*in) were obtained – a reduction of 56.7% for coulomb and an increase of 187% for resistivity. With the addition of small amounts (<5%) of silica fume and metakaolin and (<35%) GGBFS, the AASHTO T277 measurement decreases significantly and the resistivity inversely. The microstructure becomes more dense as the calcium hydroxide is consumed by the pozzolans, making it more difficult for the chloride ions and electrical current to pass through the concrete.

Effects of Different Pozzolans

Although mixtures contained different amounts of pozzolans, Fig. 5.5 to Fig. 5.10 illustrate that there is a general trend in most of the pozzolans used in this study. Each of

the Figs. 5.5 to Fig. 5.10 shows the theoretical line for reference from all mixtures and each pozzolan that was used and where the data plotted compared to the theoretical line. Silica fume can be found in Fig. 5.5, which shows that the addition of silica fume (3-5% in this case), lower values of C1202 and higher resistivity readings are obtained. Those familiar with C1202 may notice that the values appear to be higher than expected (expected less than 1,000); this appears in mixtures containing Class F fly ash and less than 5% silica fume. This combination of Class F fly ash and silica fume is less resistant to chloride ion penetration as compared to the other mixtures containing silica fume.

Similar to silica fume, Fig. 5.6 shows that with the addition of Metakaolin (3-5%), the coulomb values are on the lower end of the range of data obtained. In Fig. 5.7, slag mixtures are presented again with coulomb values on the mid to lower end of the range. In Fig. 5.8, Class F fly ash varied from the mid to upper end of the theoretical line. This is possibly due to excess bleed water forming additional voids in the concrete. In Fig.

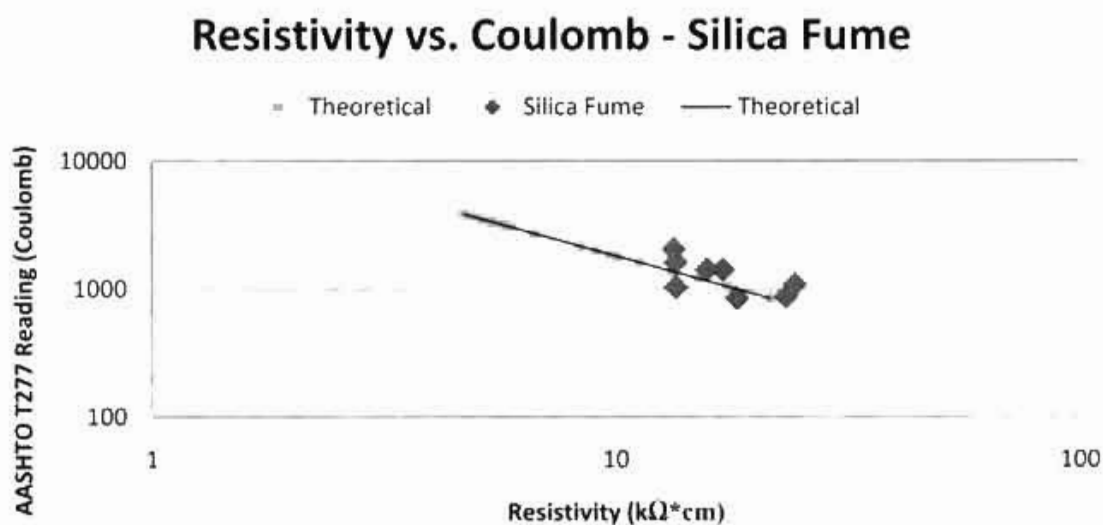


Fig. 5.5—AASHTO T277 coulomb vs. Wenner resistivity – silica fume

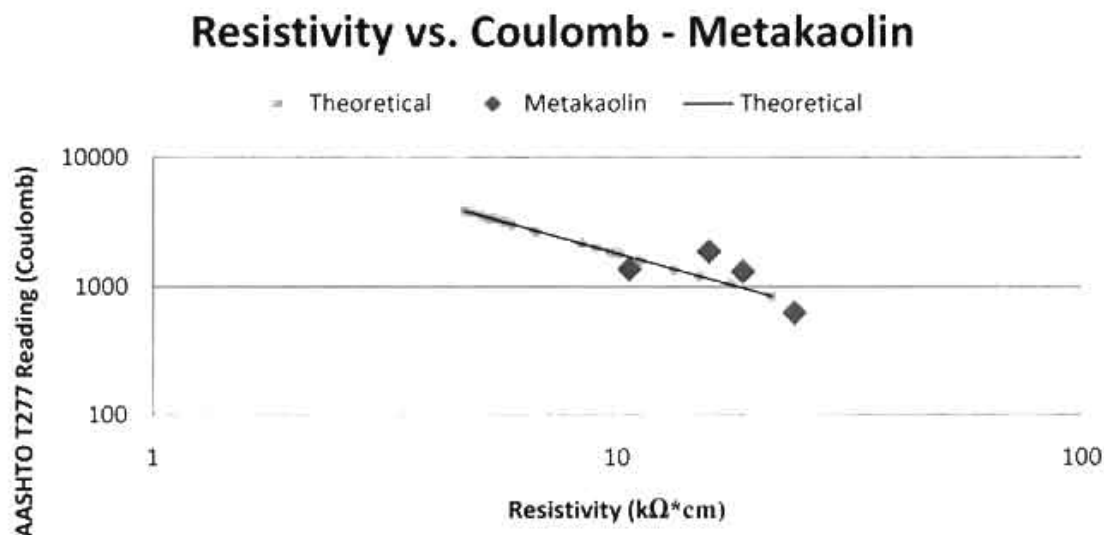


Fig. 5.6—AASHTO T277 coulomb vs. Wenner resistivity - metakaolin

5.9, another Class F fly ash (designated F2) with a similar trend to the previous Class F fly ash is observed. Fig. 5.10 shows the Class C fly ash on the upper end of the theoretical relationship. Again, this is most likely due to excess bleed water caused by the fly ash.

As seen in Fig. 5.8 and Fig. 5.9, one of the largest variations in C1202 data and resistivity was using the two Class F fly ashes. Again, this was possibly due to excess water and bleeding caused by the fly ash. In general, a good correlation in resistivity and C1202 was obtained.

Suggested Additional Research

Geometric Correction Factor

The geometric correction factor established by others (9) was established using Type I, Type I with 20% fly ash, and Type II cements. These generally have higher

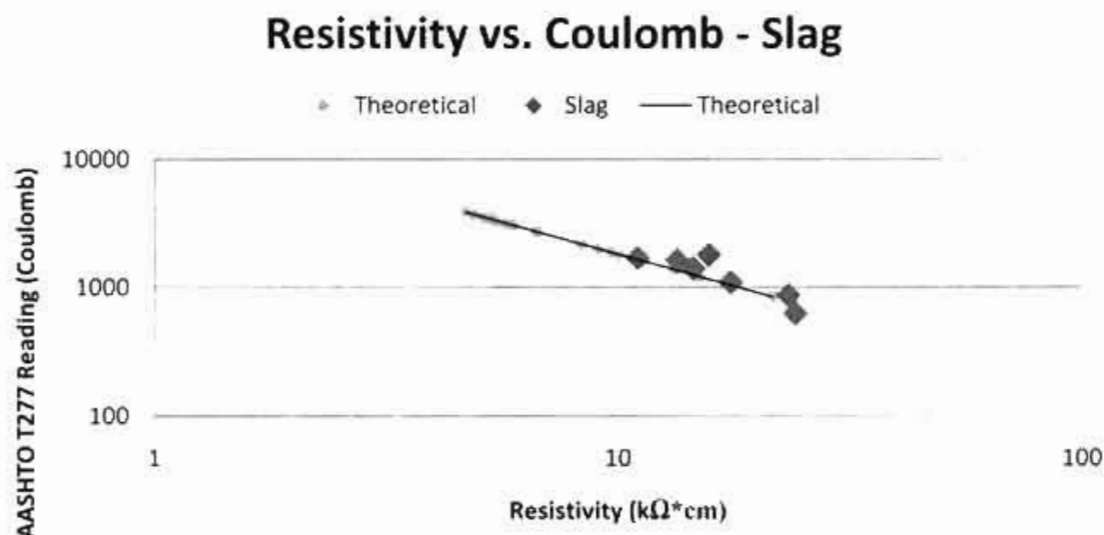


Fig. 5.7—AASHTO T277 coulomb vs. Wenner resistivity – slag

permeability as compared to mixtures containing silica fume or slags. It was observed from information collected by others (14) that there appeared to be different variations between the cylinder resistivity and the slab resistivity depending on the permeability of the mixture. Mixtures with lower resistivity were close to 2.7 as was used throughout this thesis, but those with higher permeability are significantly higher (closer to 3.3). The testing device was similar to the one used in the tests for this thesis. Information in Table 5.4 was taken from Smith (14) and shows the comparison of the different mixture resistivity for slabs and cylinders and the correction factor needed to obtain the slab resistivity from the cylinder resistivity. In Table 5.4, PC is portland cement, BS is ground granulated blast-furnace slag, SF is silica fume, and FA is Class F fly ash.

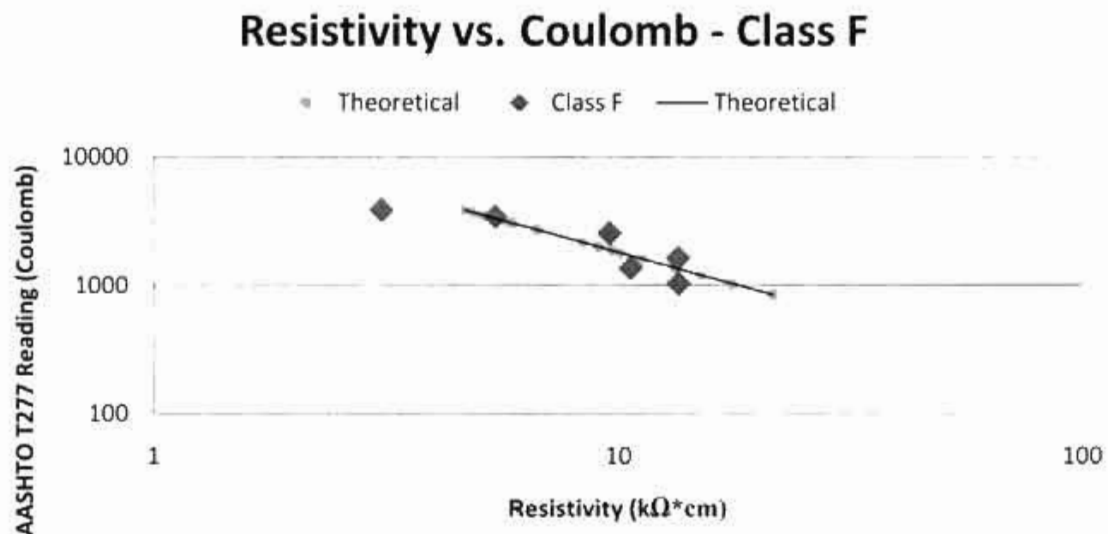


Fig. 5.8—AASHTO T277 coulomb vs. Wenner resistivity – Class F fly ash

Resaturation

Data has been collected on different curing methods and their effect on resistivity. One of the main reasons for this procedure was to determine if it is possible for the concrete to be resaturated after it has been dry cured for a period of time. As stated in Chapter 3, all specimens used in this thesis were wet cured until the day of testing. Other specimens were wet cured until 14 days, then removed for dry cure until the time of testing. These specimens were tested at 2 days, 14 days, 28 days, and 98 days after being cast.

Two drying schemes were established after the 14th day of wet curing. The first was to dry cure the specimen until 2 days before testing, then place the cylinder in wet cure and test on the prescribed days. This information could then be compared to the wet curing resistivity data. The other drying scheme involved dry curing until 3 days before testing, then placing the cylinders in wet cure until the day of testing. Again, this

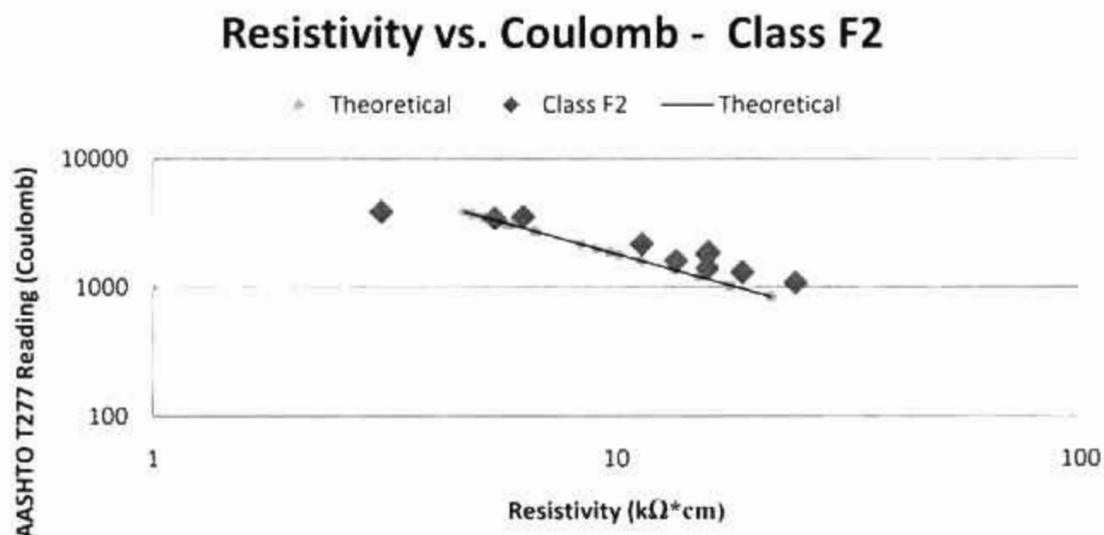


Fig. 5.9—AASHTO T277 coulomb vs. Wenner resistivity – Class F2 fly ash

information would need to be compared to the wet cured specimens. Through this variation in drying methods, it was anticipated that that data would indicate whether it was possible to resaturate the cylinders after a drying period. Obviously, there are other variations that could affect the resistivity readings, so other tests would need to be performed to determine the saturation level of the concrete. Determining the saturation level and establishing a method to resaturate concrete in-situ and a level of saturation that is adequate for the resistivity meter to work properly would be an area of future work. This needs to be completed before Wenner resistivity can realistically be used in- situ. In the meantime, as expressed in other areas of this thesis, cylinders could be cast and left in wet cure until the day of testing.

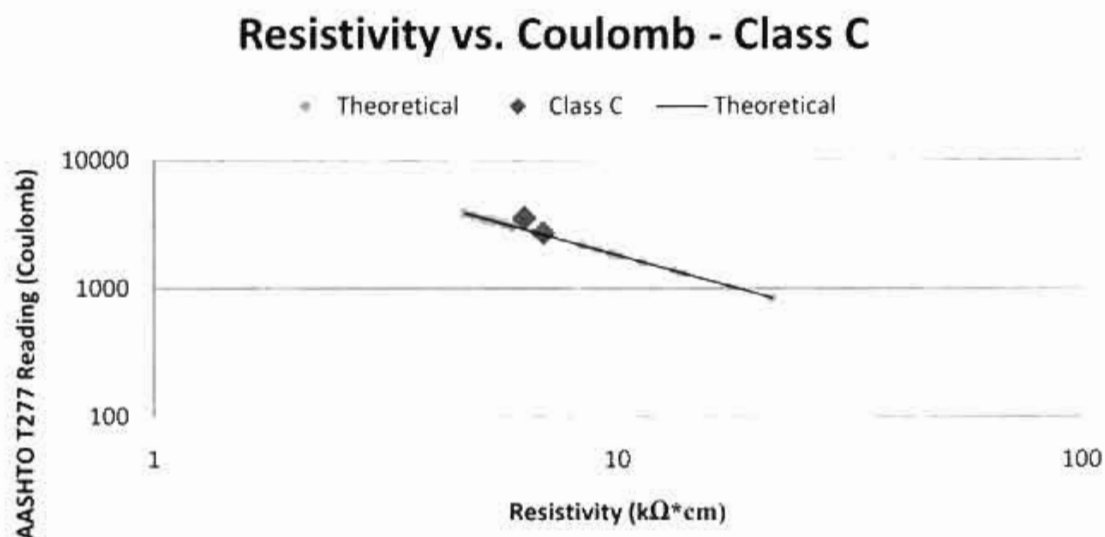


Fig. 5.10—AASHTO T277 coulomb vs. Wenner resistivity – Class C fly ash

Environmental Effects on Resistivity

Additional research should be conducted to determine how environmental factors (humidity, solar heating of concrete, temperature) affect resistivity readings in-situ. If needed, adjustments should be made to resistivity readings taken in-situ to compare with lab-based ASTM C1202 readings.

Prediction Testing

Additional analysis and testing may be considered for early predicting of concrete permeability at 28 days for 98-day characteristics. If a reliable correlation were to exist between the 28-day resistivity and 98-day permeability data, it would allow the resistivity meter to be used as a quality control measure earlier than the 98 days presented, and would capture the effects of the pozzolans on permeability. This would also allow the testing to be completed before traffic and deicing salts are applied to the structure. Fig.

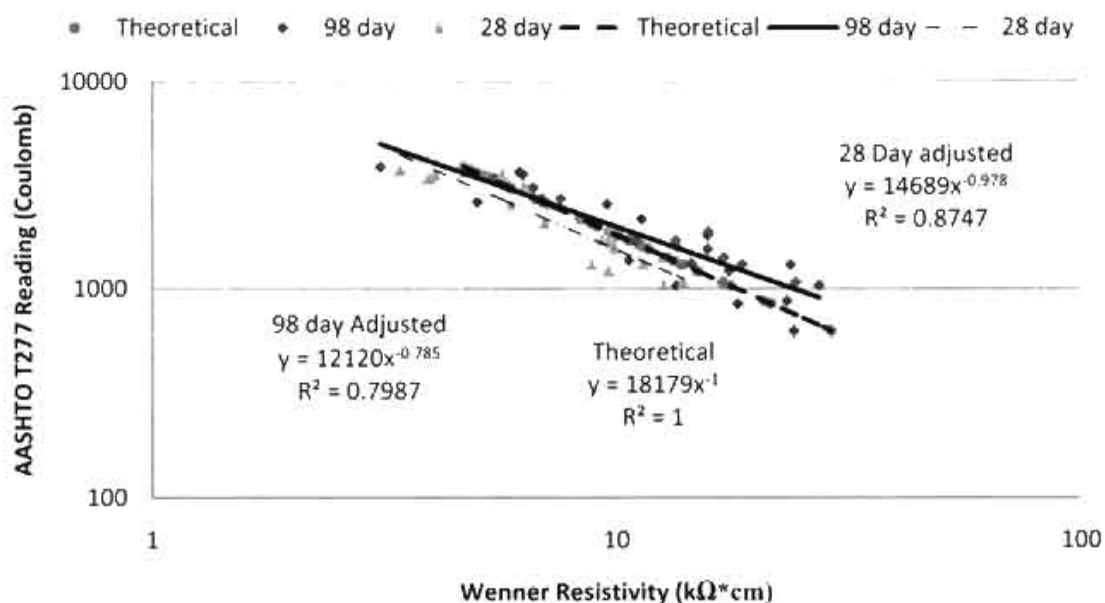
Table 5.4 – Correction factor variability

Test #	Mixture Composition	Cylinder Resistivity (kΩ*cm)	Slab Resistivity (kΩ*cm)	Correction Factor Required
1	100PC(0.54w/c)	15.5	5.8	2.67
2	97PC/3SF(0.57wc)	26.3	5.3	4.96
3	100PC	19.3	7.5	2.57
4	100PC	16.5	6.4	2.57
7*	70PC/27FA/3SF	58.0	17.5	3.31
10*	70PC/30FA	44.0	10.6	4.15
11	65PC/30FA/5SF	91.0	21.2	4.29
12	97PC/3SF	33.5	10.4	3.22
13	65PC/35BS	49.0	14.9	3.29
14**	55PC/42BS/3SF	99.0	28.7	3.45
15	100PC	17.9	6.9	2.59
16	55PC/42BS/3SF	65.6	29.8	2.20
17	70PC/27FA/3SF	35.6	22.4	1.59

* indicates a gap in testing numbers due to missing cylinder data

** Capacity of meter exceeded

Wenner Resistivity vs. T277 Coulomb

**Fig. 5.11—98-day AASHTO T277 coulomb vs. 28-day Wenner resistivity**

5.11 is a plot of the 28-day wet cured resistivity vs. 98-day ASTM C1202 chloride ion permeability. There is a good correlation in this data ($R^2 = 0.87$). A better correlation should try to be obtained to see if using resistivity readings at 28 days as a predictor of 98-day durability is justified.

CHAPTER 6

SUMMARY AND CONCLUSIONS

Summary

Research was conducted to determine the electrical resistivity of the concrete using ASTM C1202. Electrical resistivity is a physical property that indicates how strongly a material opposes the flow of electric current. A low resistivity indicates that the current can flow through the material with relative ease; conversely the higher the resistivity, the more opposition the current experiences through the material. It considers the electrical resistance, cross-sectional area of the specimen, and the length through which the current must pass. In concrete, resistivity is related to how interconnected the voids are, the amount of ions present, and the amount of saturation.

The research also involved determining the electrical conductivity of the concrete according to ASTM C1202. Electrical conductivity is the inverse of electrical resistivity, and is the type of measurement performed when using the ASTM C1202 testing method. When high conductivity concrete is used in construction where rebar and chlorides are present, a faster deterioration of rebar occurs as compared to low conductivity concrete.

Electrical resistivity and electrical conductivity are related through Ohms law. Ohms law states that current flowing in a material is directly proportional to the potential difference across the ends of a resistor divided by the resistance of the resistor. The

current is transported by ions present in an electrolyte, which in this case is the fluid found inside the concrete specimen. In concrete, there are a series of voids created by the hydration process and these voids become saturated with hydroxyle and chloride ions when exposed to chlorides. These series of voids allow the current to pass through the concrete, and the electrolytes make it possible to use Ohms law to relate electrical tests with each other.

It has been shown that there is a correlation between the testing results of ASTM C1202 and Wenner resistivity using Ohms law. This correlation was made using two correction factors, one to account for the joule effect in the ASTM C1202 method, and the other to account for geometric differences in the resistivity method. The result bridges the gap between these two testing methods and shows scientifically through physics that there is another method for electrical indication of chloride ion ingress in concrete.

Additional research needs to be completed to improve the reliability of the relationship in order to further improve the quality control of concrete. More research should also be completed on how to implement these testing methods in the field.

Conclusions

An excellent relationship between the two testing methods has been developed, and it is considered to be valid based on the correlation of the data presented. This is particularly true for mixtures with higher permeability. More research should be conducted to further correlate this data with low permeability mixtures.

By using adjustments for cylinder geometry for resistivity and the joule effect during testing for T277, it is possible to obtain resistivity measurements from a 10 cm by 20 cm (4 inch by 8 inch) cylinder and compare them to theoretical resistivity data obtained by using AASHTO T277. These factors were verified through independent testing. Through the use of these factors, it is possible to obtain correlations for ternary mixture, binary mixture, and unblended cement concretes.

This data supports the use of the Wenner device as a quality assurance/quality control (QA/QC) tool in concrete field testing. To be used in the field for in-situ testing, additional research should be conducted to determine the effect of the concrete and saturation solution temperature on resistivity readings and, if needed, a correction be developed. In addition, a testing method needs to be developed that specifies the dry curing period between wet curing and the time of testing in order to standardize and compare the results. Continued research into how to ensure that concrete in the field is saturated to an acceptable level (saturated surface dry [SSD]) should be performed as well as environmental effects on resistivity readings in-situ. Cylinders cast as QA specimens and placed in wet curing for strength testing could be used for resistivity testing.

Consistent testing methods should be followed in order to obtain correct correlations. Through testing it was found that resistivity readings taken at 5 minutes as compared to those taken at 45 minutes after being removed from wet cure are approximately 15% lower, and compared to 60 minutes are approximately 25% lower. This shows that testing in a fully saturated condition is necessary and there is a need for standardization in order to obtain reliable correlations.

Well-proportioned concretes containing pozzolans such as Class F fly ash, Class C fly ash, silica fume, metakaolin, and ground granulated blast furnace slag will yield concrete more resistant to chloride ion penetration and resistance to electrical current. As shown, with the substitution of only a small amount of silica fume (3%) or ground granulated blast furnace slag (35%), a great reduction in the chloride ion ingress can be accomplished.

APPENDIX

98-Day Resistivity and Coulomb Data

As stated earlier in this thesis, the blends of cement include pozzolans such as silica fume (SF), ground granulated blast furnace slag (GGBFS), two types of Class F fly ash (labeled F and F2), Class C fly ash, and metakaolin. In addition to different types of pozzolans, different types of cements were used including type IP (portland-pozzolan), type IS (portland blast-furnace slag), type ISM (slag-modified portland cement), and type E (as defined in this research, limestone). These abbreviations are used next to percentages of each mineral admixtures (i.e., 75TI/20F2/5M indicates 75% type I, 20% F2 fly ash, and 5% Metakaolin). Tables A.1 and A.2 contain the summarized data used in this research for 98-day and 28-day testing.

Table A.1 – Condensed 98-day resistivity and coulomb data

Mix ID	Wet Cure 98-day Resistivity	Number of Readings	Standard Deviation	Geometric Adjusted Resistivity	ASTM C1202 Data	Temp Adjusted C1202
	k Ω *cm			k Ω *cm	Coulombs	Coulombs
75TI/20F/5M	28.69	16	4.50	11	1621	1369
60TI/30F/10F2	8.38	16	1.27	3	6786	3871
60TI/20F2/20G120S	42.38	8	5.26	16	2316	1804
75TI/20F2/5M	42.63	8	3.25	16	2364	1877
67TI/30F2/3SF	36.31	16	6.55	13	1988	1611
60TI/20F/20F2	14.75	8	3.11	5	5490	3431
100TIP	20.50	8	7.75	8	4023	2715
60TI/30F2/10	17.00	8	1.93	6	6137	3558
75TISM/25C	18.66	16	4.36	7	4024	2725
75TISM/25F2	30.63	16	3.56	11	3032	2173
97TISM/3SF	49.25	16	6.83	18	935	845
75TI/20F/5SF	36.38	8	3.11	13	1163	1032
100TI	17.88	16	2.39	7	4563	3068
65TI/30F2/5SF	64.0	16	9.24	24	1512	1308
65TIP/35G120S	73.75	16	10.96	27	1176	1040
60TI/20F/20G120S	36.25	16	4.71	13	2000	1709
100E	16.71	48	1.05	6	5890	3649
80E/20G120S	29.75	48	6.02	11	1970	1703
95E/5SF	45.96	48	6.92	17	1657	1415
75TI/20F2/5M	50.38	16	8.28	19	1568	1314
62TI/35G120S/3SF	62.81	16	12.89	23	985	872
60TI/35G120S/5M	65.06	16	8.23	24	698	627
100TI	13.56	16	2.72	5	3814	2619
75TI/20F2/5SF	65.63	16	5.50	24	1230	1071
77TI/20F2/3SF	42.41	32	4.10	16	1900	1555
65TISM/35G120S	39.19	16	2.01	15	1568	1318
50TI/35G120S/15F	47.19	16	4.12	17	1438	1216
85TIP/15F	25.81	16	1.83	10	3634	2555
Number of readings taken (8 per cylinder)†						

28 Day Resistivity and Coulomb Data

Table A.2 – Condensed 28-day resistivity and coulomb data

Mix ID	Wet Cure 98-day Resistivity	Number of Readings	Geometric Adjusted Resistivity
	kΩ*cm		kΩ*cm
75TI/20F/5M	19.19	16	7.11
60TI/30F/10F2	6.48	16	2.40
60TI/20F2/20G120S	19.88	8	7.36
75TI/20F2/5M	22.75	8	8.43
67TI/30F2/3SF	19.25	16	7.13
60TI/20F/20F2	9.51	8	3.52
100TIP	12.75	8	4.72
60TI/30F2/10	10.16	8	3.76
75TISM/25C	10.25	16	3.80
75TISM/25F2	13.75	16	5.09
97TISM/3SF	23.75	16	8.80
75TI/20F/5SF	15.38	8	5.69
100TI-AG	12.32	16	4.56
65TI/30F2/5SF	23.88	16	8.84
65TIP/35G120S	34.12	16	12.64
60TI/20F/20G120S	N/A	N/A	N/A
100E	12.73	48	4.71
80E/20G120S	25.17	48	9.32
95E/5SF	33.98	48	12.58
75TI/20F2/5M	N/A	N/A	N/A
62TI/35G120S/3SF	N/A	N/A	N/A
60TI/35G120S/5M	N/A	N/A	N/A
100TI	N/A	N/A	N/A
75TI/20F2/5SF	37.69	16	13.96
77TI/20F2/3SF	26.81	32	9.93
65TISM/35G120S	30.81	16	11.41
50TI/35G120S/15F	25.94	16	9.61
85TIP/15F	16.06	16	5.95
Number of readings taken (8 per cylinder)↑			

REFERENCE

1. ASTM Standards vol. 04.01, 04.02, American Society for Testing and Materials, Philadelphia, PA, 2007.
2. AASHTO Standard T277, "Standard Method of Test for Electrical Indication of Concrete's Ability to Resist Chloride," American Association of State Highway and Transportation Officials, Washington, D.C., U.S.A, 2005.
3. Mehta, P., and Monteiro, P., "Concrete Microstructure, Properties, and Materials," 3rd Edition, McGraw-Hill Professional, New York, NY, USA, 2006, 177-182. Print.
4. Ewins, A.J. "Resistivity Measurements in Concrete," *British Journal of NDT*, V. 32, No. 3, 1990, pp. 120-126. Print.
5. Serway, R., and Jewett, J., "Physics for Scientists and Engineers, with Modern Physics," 6th Edition, Thomson Brooks/Cole, Belmont, CA, USA, 2004, pp. 835-837. Print.
6. Feldman, R.F., Chan, G.W, Brousseau, R.J., and Tumidajski, P.J., "Investigation of the Rapid Chloride Permeability Test," *ACI Materials Journal*, V. 91, No. 2, 1994, pp. 246-255.
7. Gowers, K.R., and Millard, S.G., "Measurement of Concrete Resistivity for Assessment of Corrosion Severity of Steel Using Wenner Technique," *ACI Materials Journal*, V. 96, No. 5, 1999, pp. 536-541.
8. Sengul, O., and Gjorv, O.E., "Electrical Resistivity Measurements for Quality Control During Concrete Construction," *ACI Materials Journal*, V. 105, No. 6, 2008, pp. 541-547.
9. Morris, W., Moreno, E.I., and Sagües, A.A., "Practical Evaluation of Resistivity of Concrete in Test Cylinders using a Wenner Array Probe," *Cement and Concrete Research*, Vol. 26, No. 12, 1996, pp. 1779-1787.
10. Kessler, R.J., R.F. Powers, and M.A. Paredes. "Resistivity Measurements of Water Saturated Concrete as an Indicator of Permeability," *NACE International Corrosion Conference 2005*, Houston, Texas, Paper 5261, pp. 1 – 10.

11. FDOT Standard FM5-578, "Florida Method of Test for Concrete Resistivity as an Electrical Indicator of Its Permeability," Florida Department of Transportation, 2004.
12. Julio-Betancourt, G.A., and Hooton, R.D., "Study of the Joule Effect on Rapid Chloride Permeability Values and Evaluation of Related Electrical Properties of Concretes," *Cement and Concrete Research*, V. 34, 2004, pp. 1007 - 1015.
13. Wee, T.H., Suryavanshi, A.K., and Tin, S. S., "Evaluation of Rapid Chloride Permeability Test (RCPT) Results for Concrete Containing Mineral Admixtures," *ACI Materials Journal*, V. 97, No. 2, March-April 2000, pp. 221 - 232.
14. Smith, K., "Evaluating Concrete Bridge Design Factors Using Concrete Resistivity," Penn State University Master's Thesis, 2002, pp. 92-113, pp. 151-152.
15. Stanish, K.D., Hooton, R.D., and Thomas, M.D.A., "Testing the Chloride Penetration Resistance of Concrete: A Literature Review," FHWA Contract DTFH61-97-R-00022 University of Toronto, Toronto, Ontario, Canada. June 31, 2000.
16. Berke, N. S., and Hicks, M.C., "Estimating the Life Cycle of Reinforced Concrete Decks and Marine Piles Using Laboratory Diffusion and Corrosion Data", *Corrosion Forms and Control for Infrastructure*, ASTM STP 1137, V. Chaker, ed., American Society for Testing Materials, Philadelphia, 1992.
17. Tikalsky, P., Schaefer, V., Wang, W., Scheetz, B., Rupnow, T., St. Clair, A., Siddiqi, M., and Marquez, S., "Development of Performance Properties of Ternary Mixtures: Phase I Final Report," Report No. Pool Fund Study TPF-5(117). Federal Highway Administration. Washington, DC. December 2007.
18. Rupnow, T. D., Schaefer, V. R., Wang, K., and Tikalsky, P. J., "Effects of Different Air Entraining Agents (AEA), Supplementary Cementitious Materials (SCM), and Water Reducing Agent (WR) on the Air Void Structure of Fresh Mortar," International Conference on Optimizing Paving Concrete Mixtures and Accelerated Concrete Pavement Construction and Rehabilitation, FHWA/ACI/ACPA, Nov. 6-9, 2007.